



UNIVERSITY OF NAIROBI
FACULTY OF ENGINEERING
DEPARTMENT OF ENVIRONMENTAL AND BIOSYSTEM ENGINEERING

***OPTIMIZING BIOGAS UPGRADING IN A PACKED COLUMN
BY ENHANCING MASS-TRANSFER OPERATION***

BY

MARTIN KEMBOI
(F56/87467/2016)

(B. Tech, Chemical and Process Engineering, Moi University, Kenya).

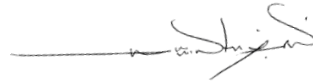
**A thesis submitted in partial fulfillment for the Degree of Master of Science
in the Environment and Biosystem engineering
in the University of Nairobi**

December 1, 2021

**

DECLARATION/APPROVAL

This thesis is my original work
and has not been presented for a degree in any other university.



MARTIN KEMBOI

Date: September 16, 2021

This thesis has been submitted for examination with our approval as university supervisors

- 1) Dr. Duncan O. Mbuge

Sign: 

Date: 21st September 2021

- 2) Mr. Januarius O. Agullo

Sign: 

Date: 21st September 2021

**

*"I would like to dedicate my work to God almighty.
My profound gratitude goes to
my wife Beatrice and daughter Ella.
Due to your encouragement, tenacity has been sustained.
I now have another reason to inquire further."*

**

ACKNOWLEDGEMENTS

I would like to express my gratitude to my primary advisor, Dr. Duncan O. Mbuge, for his timely guidance from the inception of the project. Your initial analysis of the original concept has brought me to where I am and I don't take that for granted. I would also like to acknowledge the constructive criticism I received from my second advisor Mr. Januarius O. Agullo who made me burn the mid-night oil.

I wish to acknowledge the entire staff of the mechanical engineering laboratory of the University of Nairobi, who provided space and technical support making the realization of my goals come to pass. In this regard I would like to recognize the support I received from the lab technicians Mr. Jacton Anyona. You made me.

**

Biogas is a gas produced by decomposition of organic matter by microorganisms in an environment devoid of oxygen via hydrolysis, acidobenesis, acetogenesis and methanogenesis. Biogas is mainly made up methane and carbon dioxide, whose proportions vary depending of the substrate used and the condition in the bio-digester. Due to the presence of carbon dioxide, raw biogas contributes to global warming and lowers the calorific value of the utility gas while the trace element hydrogen sulfide, is not only a corrosive gas, but a health hazard to the handlers. This increases storage and handling costs and costs, the costs incurred when seeking medical attention. To its calorific value, the gas is upgraded from one of a modest methane content of 40 to 60% to biomethane of more than 95% methane by sequestering carbon dioxide and hydrogen sulfide in processes like physical absorption, chemisorption, pressure swing adsorption and membrane separation.

The objective of this investigation is to optimizes biogas upgrading in a packed column by enhancing mass transfer of CO₂ molecules across the phases. The absorption is enhanced by the chemical reaction between CO₂ reacts with dilute aqueous sodium hydroxide solution in the liquid phase. In the absorption, the effects of four non-associating factors on the overall mass transfer coefficient were separately investigated using the ratio of carbon dioxide mole fraction in the gas feed to the column to that of the effluent gas. This was done by varying one factor while keeping the other factors constant and the overall mass transfer coefficient $K_y a_e$, ccalculated. The factors considered were the gas superficial velocity u_y , the solvent superficial velocity u_x , solvent concentration C_x and carbon dioxide mole fraction in the gas feed to the column y_a . Using the $L_9 3^4$ orthogonal array of the Taguchi method of optimization, the column's optimum operating condition was established. This was achieved by transforming the overall mass transfer coefficient for each trial to the signal-to-noise ratio (ψ) using the "larger-the-better" objective function.

The results showed that the optimum operating condition of posted a signal-to-noise ratio of -1.5539 , which is equivalent to an the overall mass transfer coefficient of $0.8444 \text{ mol}/\text{m}^3 \cdot \text{s} \cdot \text{Pa}$. It was also found that the influence of the factors on the response parameter was in the order $u_x > C_x > y_a > u_y$ where the influence of y_a and u_y on the absorption process is insignificant. This trend implies that CO₂ flux across the gas-liquid interface is greatly influenced by the effective area a_e , that is a function of turbulence in the liquid phase. The finds here can applied in biogas production units where the column is directly connected to the raw gas line from the digester, and operated with a high liquid-to-gas (L/G) ratio. The high ratio would be sufficient in eliminating the

need of chemisorption thereby making the process a purely a physical process while still retaining the benefits of eliminating the health hazard associated with biogas, increase its calorific value and reduce CO₂ emission a remedy of global warming.

Keywords: - *Biogas, absorption, overall mass transfer coefficient, carbon dioxide, packed column, Taguchi method, solvent superficial velocity.*

**

TABLE OF CONTENTS

DECLARATION/APPROVAL.....	i
ACKNOWLEDGEMENTS.....	iii
ABSTARCT.....	iv
TABLE OF CONTENTS.....	vi
LIST OF FIGURES.....	viii
LIST OF TABLES.....	ix
NOTATIONS.....	x
ABBREVIATIONS.....	xii
CHAPTER ONE-INTRODUCTION.....	1
1.1. Background	1
1.2. The problem statement	2
1.3. Justification	4
1.4. Objectives	4
1.4.1. Overall objectives	4
1.4.2. Specific objectives	4
1.5. The Scope and Limitations	5
CHAPTER TWO-LITERATURE REVIEW.....	7
2.1. Introduction	7
2.2. Biogas production process	7
2.3. Upgrading	8
2.4. The choice of solvent	9
2.5. Process optimization	11
2.6. Conclusions	11
CHAPTER THREE- THE THEORETICAL FRAMEWORK.....	22
3.1. An overview	22
3.2. Chemical kinetics of absorption process	22
3.2.1. The diffusion coefficients	22
3.2.2. The reaction mechanism	22
3.2.3. The reaction rate constant	23
3.2.4. Henry’s law constant	24
3.3. Mass transfer models	25
3.3.1. The two film theory	25
3.3.1.1. Films resistances in physical absorption	25
3.3.1.2. Films resistances in chemisorption processes	28
3.3.2. The Effective mass transfer area	31
3.3.3. The overall mass transfer coefficient	31
3.4. Process optimization	32
3.4.1. The Taguchi philosophy	32
3.4.2. Experimental planning	33
3.4.2.1. The design of experiments	33
3.4.2.2. Selection of the Orthogonal Array	34
3.4.2.3. Quality loss function	34
3.4.3. Steps in optimization process	35
3.4.4. ANOVA and its significance	36

3.5. Mathematical modelling	37
3.5.1. An overview	37
3.5.2. Model development.....	38
3.5.3. Solution of the CDR equation	41
CHAPTER FOUR-MATERIALS AND METHODS	48
4.1. Introduction.....	48
4.2. Apparatus and materials.....	48
4.3. Experimental setup	49
4.4. Effective Area and Overall Mass Transfer coefficient	50
4.5. Process Optimization	51
4.5.1. Parameter identification	51
4.5.2. The experimental runs.....	51
4.5.3. The analysis of the response parameters.....	51
4.6. Calorific value measurement	52
CHAPTER FIVE-RESULTS AND DISCUSSIONS	54
5.1. A general view	54
5.2. The fractional effective Mass Transfer area.....	54
5.2.1. Effect of solvent superficial velocity	54
5.2.2. Effect of Gas Superficial Velocity.....	55
5.2.3. Effect of Solvent Concentration	56
5.2.4. Effect of carbon dioxide mole fraction	56
5.3. The Overall Mass Transfer Coefficient.....	57
5.3.1. Effect of solvent superficial velocity	57
5.3.2. Effect of gas superficial velocity.....	58
5.3.3. Effect of Solvent Concentration	58
5.3.4. Effect of Carbon Dioxide Mole Fraction.....	59
5.4. Process optimization	60
5.5. The calorific value.....	63
5.6. Column simulation.....	63
5.7. Hydrogen Sulphide sequestration.....	65
CHAPTER SIX: - CONCLUSIONS AND RECOMMENDATIONS	66
6.1. Conclusions.....	66
6.2. Recommendation	67
6.2.1. Recommendations for work done	67
6.2.2. Recommendation for future work	67
REFERENCES	69
APPENDICES.....	81
Appendix A: Parameters for the solvent.....	81
Appendix B: Gas-Solvent reaction mechanism	82
Appendix D: The column simulation code.....	84

**

LIST OF FIGURES

Figure 1.1: Global anthropogenic carbon dioxide emission in the last 60 years.....	
Figure 3.1: Types of problems and the respective signal-to-noise ratio.....	34
Figure 4.1; Flow chart for biogas upgrading process	50
Figure 5.1: Variation of the effective area with the solvent superficial velocity at three different gas superficial velocities.....	54
Figure 5.2: The variation of fractional effective area a_f with the gas superficial velocity (u_y).....	55
Figure 5.3: A plot of the variation of fractional effective area with the solvent concentration at three different solvent superficial velocities.	56
Figure 5.4: Variation of the effective area with CO2 mole fraction in the gas feed y_a	57
Figure 5. 5: Variation of the overall mass transfer coefficient with the solvent superficial velocity u_x	57
Figure 5. 6: Plot of the variation of the overall mass transfer with the gas superficial velocity u_y	59
Figure 5. 7: Plot of the variation of K_{yae} with the solvent concentration, OH –	59
Figure 5. 8: Plot of the effect of CO2 mole fraction on the overall mass transfer coefficient K_{yae} , at three different solvent velocities.	60
Figure 5. 9: Plots of the variation of the signal-to-noise ratios ψ , for the main effects for the experimental factors.	62
Figure 6. 1: Schematic representation of the elements in the computational domain.	38
Figure 6. 2: Simulated values of the variation of CO2 with gas superficial velocity, y_{CO2}	64
Figure 6. 3: Comparison of experimental and simulated effluent CO2 mole fraction $y_{CO2}(b)$ with increase in gas superficial velocity.....	65

**

LIST OF TABLES

Table 1. 1: Composition of biogas, showing the gas compositions from three different feedstock	2
Table 1. 2: A COMPARISON OF SOME PARAMETERS OF BIOGAS AND BIOMETHANE	3
Table 3.1: Types of problems and the respective signal-to-noise ratio.....	35
Table 4.1: Operating range for the experimental factors	49
Table 5.1: The response parameters in an 1934 orthogonal array.....	59
Table 5.4: The anova table.....	60

**

NOTATIONS

P_c	Carbon dioxide partial pressure	$N \cdot m^{-2}$
\hat{S}_f	Correction factor for the percentage contribution	-
$\bar{\psi}_i$	Mean signal-to-noise ratio at optimum level for the i^{th} factor	-
C_c	Methane concentration	$kmol \cdot s^{-2}$
C_c^*	Liquid phase CO_2 concentration in equilibrium with the concentration in the gas phase	$kmol \cdot m^{-3}$
C_c^i	The interface CO_2 concentration	$kmol \cdot m^{-3}$
C_T	Total gas concentration	$kmol \cdot s^{-2}$
D_c	Carbon dioxide diffusion coefficient	$m^2 \cdot s^{-1}$
D_c'	Carbon dioxide diffusion coefficient in the liquid phase	$m^2 \cdot s^{-1}$
H_1'	Henry's law constant for physical absorption	$kmol \cdot m^{-3} \cdot Pa^{-1}$
H'	Henry's law constant	$kmol \cdot m^{-3} \cdot Pa^{-1}$
K_s	Summation of ionic coefficients in a system	-
K_3	Overall mass transfer coefficient based on the liquid phase concentration	$kmol \cdot m^{-2} \cdot kPa^{-1} \cdot s^{-1}$
K_3	Overall mass transfer coefficient based on gas phase partial pressure	$kmol \cdot m^{-2} \cdot kPa^{-1} \cdot s^{-1}$
K_3	Overall volumetric mass transfer coefficient	$kmol \cdot m^{-3} \cdot s^{-1} \cdot kPa^{-1}$
N_c	Carbon dioxide molar flux	$kmol \cdot m^{-2} \cdot s^{-1}$
O_i	Solvent concentration	$gmol \cdot L^{-1}$
P_c^*	Gas phase CO_2 partial pressure in equilibrium with the concentration in the liquid phase	$N \cdot m^{-2}$
P_c^i	Carbon dioxide partial pressure at the interface	$N \cdot m^{-2}$
P_a	Atmospheric pressure	$N \cdot m^{-2}$
P_f	Parentage contribution of factor f	-
P_s	Standard pressure	$N \cdot m^{-2}$
S^{ξ}	Total sum of squares	-
S^{ξ}	Sum of squares where factor f participates	-
T_a	Atmospheric temperature	K
T_s	Standard temperature	K
V_a	Atmospheric volume	m^3
C_x	Concentration of the solvent	$gmol/L$
V_f	Vance of factor f	-
a_e	Effective mass transfer area per unit volume	m^{-1}
a_f	Fractional effective area for mass transfer	-
a_r	Geometric area for the packing per unit volume	m^{-1}
c_p	Specific eat capacity	$kJ \cdot kg^{-1}$
k_c	Second order reaction rate constant	$m^3 \cdot kmol^{-1} \cdot s^{-1}$
k_c^c	The reaction rate constant at infinite dilution	$kmol \cdot s^{-1}$
k_x	Liquid film mass transfer coefficient	$m \cdot s^{-1}$
k_3	Gas film mass transfer coefficient	$m \cdot s^{-1}$
\dot{m}	Mass flow rate	$kg \cdot s^{-1}$
u_x	Solvent superficial velocity	ms^{-1}
u_3	Gas superficial velocity	ms^{-1}
y_i	Response parameter in the i^{th} experiment	-
α^-	Counter ion	-
η_t	Number of molecules of water	-
η_N	Number of molecules of aq $NaOH$ solution	-
χ_c	Carbon dioxide mole fraction	-
ψ_i	Grand mean of signal-to-noise ratio	-
Δt	change in temperature	K
Cl	Correction factor	-
F	Variance ratio	-
Z	Column height	m
H_t	Hatta number	-

N	Number of response parameters at one level	-
O_i	Free hydroxyl ions concentration	$gmol \cdot L^{-1}$
P	Operating pressure	N/m^2
Q	Calorific value	$kJkg^{-1}$
S	Column base area	m^2
T	Operating temperature	K
V	Molar volume	m^3
f	Factor	-
k	Number of factors	-
n	Number of experiments	-
q	Number of factors contributing to the response parameter	-
x	Liquid film thickness	m
y	Gas film thickness	m
z	Direction of gas diffusion	m
β	Mass transfer enhancement factor	-
σ	Standard deviation	-

**

ABBREVIATIONS

<i>CH₄</i>	Methane
<i>H₂S</i>	Hydrogen Sulfide
<i>CO₂</i>	Carbon Dioxide
<i>ERC</i>	Energy Regulatory Commission
<i>IEA</i>	International Energy Agency
<i>NEMA</i>	National Environmental Management Agency
<i>LHV</i>	Lower Heating Value
<i>HHV</i>	Higher Heating Value
<i>OA</i>	Orthogonal Arrays
<i>CNG</i>	Compressed Natural Gas
<i>STP</i>	Standard Temperature and Pressure
<i>USDL</i>	United State Department of Labor
<i>IGCC</i>	Gas combined Cycle
<i>CDR</i>	Convective-diffusive-reactive
<i>DMP</i>	discrete maximum principle

**

CHAPTER ONE-INTRODUCTION

1.1. Background

A picture of the world's energy system shows a high degree of dynamism, with dramatic falls in the cost of key renewable technologies, upending traditional assumptions on relative costs. The recent past, changes in the global energy system caused by an increase in demand of renewable energy has been realized, necessitated by the decline in the costs of technologies used in production processes. This has been brought about by a growing shift towards the use of electricity in energy provision the world over, a profound change in China's economy and energy policies that have moved consumption away from coal and the continued surge in shale gas and light oil production in the United States. The International Energy Agency (IEA) clearly puts it into perspective (IEA, 2017). Due to this scenario, stagnation has been experienced in the global carbon dioxide emission in the last four years and focus is now on clean energy production that China has been roped in.

However, the energy picture in Sub-Saharan Africa is not as bright. With a total population of 1.216 billion, 620 million have no access to electricity and nearly 780 million use hazardous and inefficient sources of energy for cooking and in the process expose women and children to the health hazards associated with the use of unclean fuels (IEA, 2014). High prices, insufficient and unreliable energy pose a challenge for those who do have access to clean/modern energy sources. Increasing access to modern and reliable energy supply can increase the economic growth in sub-Saharan Africa and improve standards of life. Although the energy resources existing in the region are more than sufficient to meet the demand, it is poorly developed and unevenly distributed necessitating the need of regional energy integration. If the abundant renewable energy potential were to be properly harnessed, we would be in a position to generate 40 percent of all our power needs from renewable sources ranging from large hydropower dams to mini-and off-grid solutions in more remote areas of the continent by the year 2040 (IEA, 2014).

In Kenya, the three main sources of energy are biomass, petroleum and electricity representing 69, 22 and 9 percent of the total energy supply respectively. The percentage of biomass is high as it is the main source of fuel for the rural population and according to the Global Legal Insights report of 2018, 83% of the population is believed to rely on biomass for energy provision. The country's vision 2030 blue print recognizes that energy is important to the economic, social and political of the country.

Although availability of improved domestic stoves in Kenya is high as compared to other countries in the region, 69 percent of all households still use open fire for cooking which is very inefficient. The

current renewable energy generation account to only 5% of the country's potential, necessitating its promotion across all sectors of society (Power Africa, 2015). In Kenya, biomass contributes 70 percent of the country's total energy demand, providing more than 90 percent of all rural household energy needs. This include charcoal, wood and agricultural waste with new frontiers being explored is the improvement of energy generation using forest and agro-industry waste like bagasse. An example is the co-generation of energy form sugarcane bagasse by the sugar industries in sugarcane growing regions of western Kenya (ERC, 2018).

Substantial amount of biogas can be produced from the country's abundant municipal and agricultural waste with projected estimates being 1,000 MW. This gas is made up of several gasses and is produced by anaerobic digestion of biomass in a bioreactor. Of the constituent gasses, methane (CH_4), and hydrogen (H_2), are the only combustible components, while carbon dioxide (CO_2) and the other minor components as the non-combustible components. Table 1.1 shows the content of biogas produced in bio-digesters using different substrates.

The primary use of the anaerobic digester (AD) is the provision of biogas used to fire domestic stoves mainly in farming communities but newly developed technologies have enabled internal combustion engines to run on purified biogas or bio-CNG (Rau *et al.*, 2017). A secondary use is in solid waste management, contributing to the global campaign against greenhouse gas emission from landfills which is a source of wild CH_4 and CO_2 . The AD have the ability to adequately manage leachate from landfills, which contaminates ground water with organic and inorganic contaminants (Mir *et al.*, 2016). For an efficient use of the biofuel, the AD must incorporate technologies for upgrading the raw gas by sequestrating CO_2 and H_2S to produce biomethane, a less harmful gas with a higher calorific value.

1.2. The problem statement

Due to the presence of CO_2 and H_2S in biogas, the efficiency of the gas is lowered and contributes to global warming as CO_2 is a greenhouse gas (GHG) and while H_2S poses a health risk to the primary user. Raw biogas has an average lower calorific value (LCV), of 19.5 MJ/kg, which is the sum of the contributions from the combustible gasses, CH_4 and H_2S . On the other hand, biomethane, purified form of biogas, has an LCV of 52 MJ/kg which is 2.7 times that that of raw biogas as presented in Table 1.2 (Green brick eco-solutions, 2014). The difference is brought about by the non-combustible components which acts as heat sinks, reducing the thermal efficiency of the combustion. Anthropogenic emission of CO_2 has grown steadily from the advent of industrial revolution leading to a considerable increase in

global temperatures. The trend is presented in 1.1. H₂S on the other hand is a corrosive gas that increases maintenance cost in machinery powered by biogas with H₂S content exceeding 100 ppm (Villanueva *et al.*, 2014). The United State Department of Labor (USDL, 2016) have set a safe concentration threshold

Table 1. 1: Composition of biogas, showing the gas compositions from three different feedstock

Component	Agricultural Waste (%)	Landfill (%)	Industrial Waste (%)	Desired Composition (%)
Methane	50-80	50-80	50-70	>70
Carbon Dioxide	30-50	20-50	30-50	<10
Water	Saturated	Saturated	Saturated	N/S
Hydrogen	0-2	0-5	0-2	<0.01
Hydrogen Sulfide	7	0-1	0-8	N/S
Ammonia	Trace	Trace	Trace	N/S
Carbon Monoxide	0-1	0-1	0-1	N/S
Nitrogen	0-1	0-3	0-1	N/S
Oxygen	0-1	0-1	0-1	N/S

Adapted from: *Removal of H₂S and CO₂ from Biogas by Amine Absorption*. by J. Huertas, I. N. Giraldo and S. Izquierdo, 2011. Automotive Engineering Research Center-CIMA of Tecnológico de Monterrey, Mexico, <http://www.intechopen.com/books/mass-transfer-in-chemical-engineeringprocesses/removal-of-h2s-and-co2-from-biogas-by-amine-absorption>, [Accessed February 5-2018].

Table 1. 2: A Comparison of some parameters of Biogas and Biomethane

	Biogas	Biomethane
Methane	55 - 65 percent	92 – 98 percent
Carbon Dioxide (v/v)	35 – 45 percent	2 – 8 percent
Hydrogen Sulfide (ppm)	500 – 30,000	< 20
Moisture (°C dew point)	Saturated	< - 40 °C
Other impurities	Present	Not Present
Calorific Value (LCV)	19,500 kJ/kg	52,000 kJ/kg

Adapted from: *Renewable Natural Gas - Bio CNG*. By Greenbrick eco-solutions, 2014. www.gbcs.in [Accessed February 3-2018]

level at 20 ppm for closed rooms. This is not met by raw biogas. Exposure to the gas at high concentration may result in loss of consciousness, coma, respiratory paralysis, seizure and the risk of spontaneous abortion or death (Kari Hemminki and Marja-Liisa Niemi, 1982; ATSDR, 2010).

These challenges can be addressed by upgrading the raw gas using processes like packed column absorption, pressure swing adoption, membrane separation, cryogenic upgrading or the in-situ methane enrichment. In all these processes, a packed absorption column is most applicable in a small biogas production plant in farming communities or institutions (Vienna Institute of Technology. 2012).

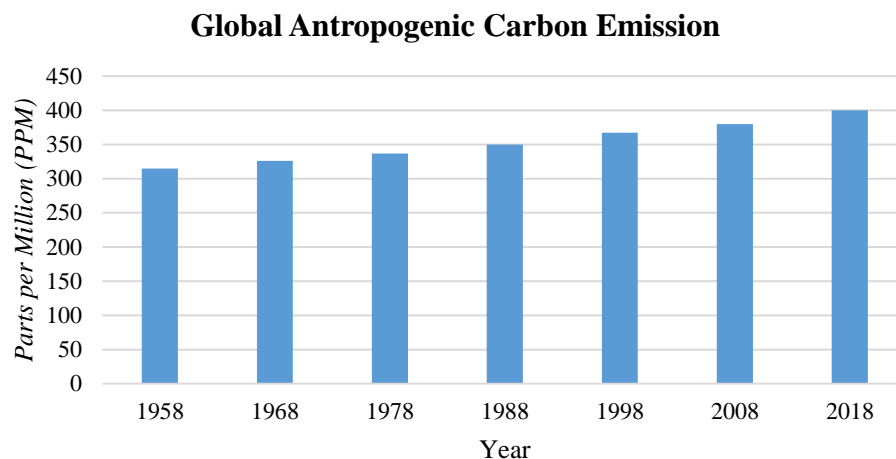


Figure 1. 1: Global anthropogenic Carbon Dioxide emission in the last 60 years. Adapted from: The National Oceanic and Atmospheric Administration (NOAA)

1.3. Justification

Biomethane, a more purified form of biogas, is a cleaner gas as it has lower carbon emission, has an increased calorific value. Due to its reduced volume and corrosively, cost associated with handling, storage and equipment maintenance will reduce considerably. It will be less harmful to the user of the utility gas thereby reduce medical bill for family units and the central government.

1.4. Objectives

1.4.1. Overall objectives

The overall objective of this study is the optimizing biogas upgrading in a packed absorption by enhancing mass transfer of CO₂ molecules.

1.4.2. Specific objectives

The following specific objectives are set in order to realize the overall objective.

- i. Evaluate the effect of the column variables on the effective mass transfer area and subsequently the overall volumetric mass transfer coefficient,
- ii. Determine the optimal combination of the select column variables that maximizes the overall volumetric mass transfer coefficient.
- iii. Compare the calorific value of the raw gas to the gas upgraded under the optimal conditions in II above.

-
- iv. Develop a mathematical model describing CO_2 profile in the packed bed as function of gas superficial velocity.

1.5. The Scope and Limitations

This experimental study investigated the effect of a set of column variables (experimental factors) on the overall mass transfer coefficient $K_y a_e$. This was done by measuring CO_2 mole fraction in the gas to and from the column and this data is used to calculate the $K_y a_e$. The effect of the individual factors forms the basis of optimization process using the Taguchi method of optimization.

Although solvents with higher enhancement factors β , are available, this experimental investigation restricted itself to aqueous sodium hydroxide solution $NaOH$, as the solvent of choice. Literature has it that high temperature and pressure increases $K_y a_e$, but this study restricted itself to operations at standard temperature and pressure STP. This restriction was necessitated by the fact that high temperature and pressure introduces an element of complexity in the column design and adoption of the technology in micro-absorption columns would not be feasible.

**

CHAPTER TWO-LITERATURE REVIEW

2.1. Introduction

Over the last few decades, anthropogenic greenhouse gas (GHG), emission has contributed to the spiraling global temperatures substantially. This, together with the economic benefits of using biomethane has made researchers embark on developing processes for biogas upgrading by employing novel technologies for CO_2 and H_2S sequestration. A literature review of biogas production and the absorption processes is given in this chapter while that of the governing principles is given in chapter four

2.2. Biogas production process.

By comparison, the tropics is richer in biomass than other geographic regions or the world, leading to large amount of biomass being generated from agricultural waste, forestry and food industries. This brings into fore the opportunity to increase energy production by conversion of the biomass into bioenergy using ADs.

In the ADs, four main reactions take place that complete biogas production process. These are hydrolysis, acidogenesis, acetogenesis, and methanogenesis (Muzaffar *et al.*, 2016). An analysis of what transpires in the bioreactor shows that the gases are formed by respiration of the decomposer microorganism acting on the substrate in an environment devoid of oxygen (Masebinu *et al.*, 2014). The conversion can be divided into four steps (Jørgensen. 2009; Grande, 2014).

- 1) Hydrolysis: Here complex organic molecules are hydrolyzed into smaller units like sugars, amino acids, alcohols and fatty acids.
- 2) Acidogenesis: Here acidogenic bacteria further breaks down the molecules into volatile fatty acids, NH_3 , H_2S and H_2
- 3) Acetogenesis: The acetanogens transform the molecules into CO_2 , H_2 and acetic acids,
- 4) Methanogenesis: Finally, methanogenic archaea transform H_2 and acetic acid into CO_2 , CH_4 and water vapor.

On average biogas produced in these bioreactors are primarily composed of 55% CH_4 , 35-45% CO_2 with smaller amounts of H_2S and ammonia (NH_3) (Kasikamphaiboon *et al.*, 2013; abdeena *et al.*, 2017). There is usually an element of stability in these ratios, however, the ratios can be varied by the conditions in the bioreactor, namely, process imbalance and the substrate composition, temperature, pH and pressure. This is why biogas from different sources show variation in CH_4 content. For substrates made up of

carbohydrates, glucose, simple sugars and large molecules such as cellulose and hemicellulose, the CH_4/CO_2 ratio in the gas is high (Orhorhoro and Atumah, 2018).

2.3. Upgrading

Upgrading is the process of increasing the CH_4/CO_2 ratio in the raw gas. This important step to be incorporated as the final step in biogas production as CO_2 acts as a heat sink during combustion of the fuel gas. The objective of upgrading is to reduce CO_2 content in the raw gas resulting in a considerable increase in LCV of the gas (Greenbrick eco-solutions, 2014). Three fully developed technologies can be used in upgrading. The first is pre-combustion capture, involving reaction of the fuel with oxygen or air and/or steam to give synthesis gas (syngas) or fuel gas composed mainly of carbon monoxide (CO) and hydrogen. The CO is then reacted with steam in a catalytic reactor (the shift converter) to give CO_2 and more hydrogen (H_2) (Jansen et al., 2015). A physical or chemical absorption process is then used to sequester CO_2 leaving behind a hydrogen-rich fuel.

The second one is oxy-combustion where combustion of the gas is done in pure oxygen from separating oxygen from air and recycled flue gas. Research has found that this technology increases the flue gas under oxy-coal combustion suggests that great potential for reducing CO_2 emission through carbon capture and storage (Hou *et al.*, 2020). This technology is more applicable in coal combustion and high capital and operating costs. The third technology is post-combustion capture where CO_2 is captured from the flue gasses generated after combustion of biogas.

Due to the corrosively and health hazards associated with H_2S the need to reduce storage and handling, and elevate the calorific value a pre-combustion is considered in this study. There are several pre-combustion methods that can be used in purifying and upgrading the raw gas. They include physical or chemical absorption, pressure swing adsorption, biological treatment and cryogenic separations (Abdeen *et al.*, 2017). The best technology to choose is based on the specific parameters at the plant such as the availability of cheap heat and the cost of electricity.

Cryogenic upgrading makes use of the distinct boiling/sublimation points of the different gasses particularly fit the separation of carbon dioxide and methane. The raw gas is cooled to the temperatures where carbon dioxide in the gas, with a sublimation point of 194.65 K, condenses or sublimates and is then separated as a liquid or a solid fraction while methane accumulates in the gas phase. High pressures and/or low temperatures are needed to sublime CO_2 when in a mixture with CH_4 . Biogas is first cooled to 17 – 26 bars and then cooled to $-25^\circ C$ where water, hydrogen sulphide, Sulphur dioxide, halogens and siloxane are removed. Further cooling is needed to remove CO_2 either as a liquid or a solid. This method is therefore energy intensive.

Pressure swing adsorption is the second most employed technology. Here, biogas is compressed to a pressure of between 4 and 10 bar and feed to a column lined with a porous adsorbent, mainly carbon molecular sieves, that selectively retain CO_2 and H_2S . leaving the column is a product rich in CH_4 .

Of these technologies, absorption in a packed column has shown great potential in upgrading biogas due to its simplicity. The process can be carried out at ambient temperature, has a relatively low pressure drop, capable of achieving high mass transfer efficiencies, has a low capital cost and occupies a small floor space.

In designing the column, accurate models are required to predict both the pressure drop and the dual mass transfer coefficients. The models are usually semi-empirical that accounts for the specific geometry of the packing (Flagiello *et al.*, 2021). The process may either be physical or chemical absorption, differentiated by the reactivity of CO_2 and the solvent molecules that affects the CO_2 flux, which is also influenced by the concentration gradient in the gas film and the effective area a_e (Coulson and Richardson, 1991, Abdeen *et al.*, 2017).

Different theories and experimental evidence on mass transfer in packed columns have been developed over the years, are specific for the type of packing used and provide the predictive correlations for the respective coefficients per unit surface area in the gas and liquid films, k_y and k_x , the effective area for mass transfer (a_e). The correlations are usually based on the average, Reynolds, Froude, Kapitza, Graetz and Weber numbers for the liquid, the Reynolds and Schmidt numbers for the gas, the characteristic dimensions of the packing i.e. the hydraulic diameter, specific volume and surface area, corrugation angle and the void fraction (Flagiello *et al.*, 2021). The physical properties of the fluids like the molecular weight, density, viscosity, surface also have an influence on the mass transfer model.

2.4. The choice of solvent

The performance of the column is based on maximization of the overall mass transfer coefficient. CO_2 absorption capacity of NaOH solution has been found to be approximately 1.4 times that of methyl-ethanolamine MEA, and in addition, NaOH is more abundant, cheaper and more familiar than MEA (Yoo *et al.*, 2013). With the gas and solvent flowing in a co-currently, negligible liquid partial pressure, it was observed above 99% level of significance, that temperature, design of the packing and the column's hydrodynamics were the only parameters that affect $K_y a_e$. Using an aqueous NH_2 solution and employing the two-film model, transfer of CO_2 molecules greatly depends on the resistance in the liquid film, and the concentration of the solvent (Nair and Selvi, 2014). The effect if the ratio of Methyl-diethanolamine/piperazine (MDEA/PZ) on the emulsion stability and CO_2 absorption in a rotary column

been investigated (Najib *et al.*, 2015). It showed that 8% v/v span-80 produces a stable emulsion able to absorb 60.3% CO_2 . In the presence of methane, 54.1 % of carbon dioxide and 13.2 % of methane was removed from the CO_2/CH_4 gas mixture. Although they concluded that the process was a promising technique for CO_2 sequestration, a considerable amount of CH_4 is absorbed along with CO_2 .

Using a mixture of piperazine and 2-amino-2-methyl-1-propanol (AMP) in a wetted sphere absorption apparatus at a flow rate in the range 0.55 to 3.35 $kMol/m^3$, a temperature range of 30 to 40°C and piperazine of concentrations 0.058, 0.115 and 0.233 $kMol/m^3$, an increase in piperazine increases the rate of absorption by increasing the enhancement factor β (Seo and Hong, 2000). This is attributed to the contribution of the zwitterions deprotonation and the direct reaction of piperazine with CO_2 .

In a physical absorption, with an increase in biogas flow rate from 1.0 to 1.5 m^3/h , the rate of absorption increased initially but decreased thereafter (Vijay *et al.*, 2006) and at a flow rate of 1.5 m^3/h and inlet pressure of 1.0 MPa, absorption of CO_2 molecules increases considerably to as high as 99% and as the pressure was increase the rate of absorption remained constant. This figure is bound to reduce when using a spray column due to its low efficiency (Lin *et al.*, 2011).

Column efficiency increases with solvent concentration but reduces with increase in gas superficial velocity and the ratio of solute to solvent have different optimum values. Increasing the solvent flow rate and the operating temperature increases $K_y a_e$ (Yincheng and Wenyi, 2011; Ndiritu *et al.*, 2013; Xu *et al.*, 2016). The same conclusion is drawn from a column packed with Sulzer DX-type packing, 2-(diethyl amino) ethanol (DEEA) as the solvent and a lean CO_2 gas (Xu *et al.*, 2016). Computer simulations have shown that of the widely used solvents, MEA solution performs better as it demonstrates desirable energy performance and resists solvent degradation (Young *et al.*, 2016). Considering CO_2 absorption vis-à-vis the concentration and temperature of the solvent for NaOH, MEA and AMP solutions, AMP solution has been found to be having a high absorption capacity (Tontiwachwuthikul *et al.*, 1992).

Although many absorption micro models assume that in the column, there exists a liquid bulk, some systems are characterized this liquid bulk. When a very thin layer of liquid flows over a solid surface, application of the penetration model with slight modification to differentiate systems with or without a liquid bulk in physical absorption and chemisorption of the first and second order reactions show that the models apply to all systems regardless of the status of the liquid bulk provided there is a substantial film thickness (Van Elk *et al.*, 2007). Application of the penetration theory and the hydrolysis reaction was faster than the contact times involved and the theory holds in columns containing spheres even if there is little mixing of the surface layers with the bulk (Lynn *et al.*, 1955).

2.5. Process optimization

The influence of any of the chosen column variable on the outcome of optimization process is evaluated using the orthogonal arrays (OA) where the order of influence is established together with the optimum conditions using the signal-to-noise ratio (ψ) observed (Nalbant *et al.*, 2007; Mehrara *et al.*, 2012; Fei *et al.*, 2013; Shahavi *et al.*, 2016; Mehryar *et al.*, 2017; Durakovic, 2017; Davis and John, 2018).

On analyzing the influence of multiple factors on the response parameter, Chen and Lin, (2018) used solvent pH, gas flow rate (Q_y), liquid temperature (T) and solvent concentration (C_x), as the experimental factors in optimizing CO₂ absorption in a packed column. Their signal-to-noise ratio analysis showed that the influence of the factors on the column performance is in the order pH > C_x > Q_y > T . In his analysis, Abdeen *et al.*, (2017) concluded that the optimum molar ratio of liquid-to-gas flow in a packed column is approximately 18.

2.6. Conclusions

From this literature review;

- i. The solvent temperature, solvent concentration, fluids volumetric flow rates and the type of packing used in the column are the most important factors to be considered when optimizing a packed absorption column.
- ii. Since temperature is an important parameter in any chemical, biological or physical processes, it greatly influences absorption of CO₂ and it varies with the type of solvent used. This is due to variation in the activation energy in the reaction between the solvent and CO₂ molecules.
- iii. High solvent flow rate increases the rate of absorption, while high gas flow rate has reduced the absorption rate.
- iv. An increase in the solvent concentration increases the rate of CO₂ absorption as the rate of diffusion of the solute molecules at the interface increases.

It has been reported that gas purity is a function of the liquid-to-gas ratio and other factors like the column height Z the gas volumetric flow rate Q_y and the pH of the solvent pH, solvent. The combination of the superficial velocities and the concentration of the streams can be considered as a gap that has not been investigated substantially. This has informed the decision to jointly investigate the four factors in optimizing biogas upgrading in a packed column

**

3.1. An overview

Kinetic separation of a gas mixture is a process that capitalizes the difference in diffusivities of the constituent gases and the preferential absorption potential by a liquid solvent. Special consideration is given to mass transfer resistance of the diffusing gas' molecules in a region adjacent to the interface between the two phases when modelling the non-equilibrium packed column using the equilibrium isotherms as the driving force (Shafeeyan *et al.*, 2014). This chapter presents the theory behind gas absorption in a packed column and the guiding principles.

3.2. Chemical kinetics of absorption process

3.2.1. The diffusion coefficients

The relative diffusivity of gasses in the gas phase and the absorption capacity of the absorbing solvent is the basis of gas separation. Molar flux N , is a parameter that is directly proportional to the diffusivity of the diffusing gas assuming that the gas is the only diffusing gas in the dispersed phase and its partial pressure gradient in the direction of diffusion z . In this case, CO_2 and its molar flux is represented by Fick's law of diffusion in Eq. 3.1 (Coulson and Richardson, 1992).

$$N_{CO_2} = -D_{CO_2} \frac{dP_{CO_2}}{dz} \quad (3.1)$$

Assuming that CO_2 and CH_4 are the only gasses in the dispersed phase, D_{CO_2} is the diffusivity, $kmol.m^{-2}s^{-1}$, for CO_2 in CH_4 , applicable in lean CO_2 concentration, dP_{CO_2}/dz is the change concentration of solute CO_2 along the distance of diffusion z , ($kmol m^{-3}m^{-1}$). However, at high concentration, the flux increases due to bulk flows in the phase and is referred to as the drift factor, which is the ratio of the total concentration of all the gasses in the gas phase to the concentration of the non-diffusing gas (C_T/C_{CH_4}). Factorizing the drift factor in the Fick's law equation, the flux is then by:

$$N_{CO_2} = -D_{CO_2} \left(\frac{C_T}{C_{CH_4}} \right) \frac{dP_{CO_2}}{dz} \quad (3.2)$$

The diffusion coefficient D_{CO_2} is specific to the composition of the gas phase and is evaluated using various predictive models like the Stefan-Maxwell hard sphere model in Eq. 3.3 (Lynn *et al.*, 1955).

$$D_{CO_2} = \left\{ \frac{(4.3 \times 10^{-4}) T^{1.5} \left(\frac{1}{M_{CO_2}} + \frac{1}{M_{CH_4}} \right)^{0.5}}{P (V_{CO_2}^{1/3} + V_{CH_4}^{1/3})^2} \right\} \quad (3.3)$$

Where T is the absolute temperature in Kelvins (K), M_{CO_2} and M_{CH_4} , are the molecular masses of gases CO_2 and CH_4 respectively, P is the operating pressure in N/m^2 , V_{CO_2} and V_{CH_4} are the respective molecular volumes obtained by Kopp's law of additive volumes. If the solvent is pure water, CO_2 diffusion coefficient is largely dependent on the operating temperature and is defined by Eq. 3.4 (Dragan, 2016).

$$\lg D_{CH_4 \cdot x}^0 = -8.1764 + \left(\frac{712.5}{T} \right) - \left(\frac{2.591 \times 10^5}{T^2} \right) \quad (3.4)$$

where $D_{CO_2 \cdot x}^0$ is the diffusivity of CO_2 in pure water,

T is the operating temperature.

In aqueous $NaOH$ solution, the diffusivity is a function of the concentration of the solvent given by Eq. 3.5.

$$D_{CO_2 \cdot x} = D_{CO_2 \cdot x}^0 \cdot \left\{ \frac{\eta_{H_2O}}{\eta_{NaOH}} \right\}^{0.637} \quad (3.5)$$

3.2.2. The reaction mechanism

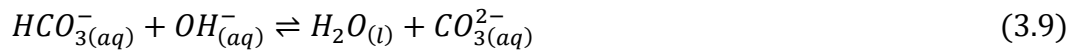
During absorption CO_2 molecules are partially transported from the bulk of the gas phase to the bulk of the liquid phase, reacting with $NaOH$ in a reaction zone which, depending on the concentration of the solvent, is located either in within the liquid film or in the bulk of the liquid. The reaction commences by physical absorption of CO_2 into the aqueous solution as given in Eq. 3.6 (Yoo *et al.*, 2012).



At the same time, the aqueous $NaOH$ solution in the liquid film, being a strong alkaline solution, dissociates into the respective ions.

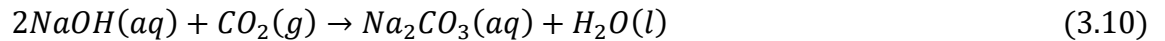


The aqueous CO_2 then reacts with the hydroxide ions to form bicarbonate and carbonate ions via Eqs. 3.8 and 3.9.



These two reactions are reversible, exothermic in the forward direction and are both characterized by high reaction rates at high pH values. Since Eq. 3.9 is instantaneous, Eq. 3.8 is considered to be rate controlling reaction (Yincheng *et al.*, 2011).

In the early stages of the absorption process, the alkalinity of the solvent makes the reaction in Eq. 3.9 predominant and increasing the concentration of the carbonate ions relative to the bicarbonate ions in the liquid phase (Yoo *et al.*, 2012). The two reactions rapidly decrease the hydroxide concentration while increasing the concentration of carbonate ions. The initial net irreversible reaction is of the second order given by Eq. 3.10 (Yincheng *et al.*, 2011).



However, with time, more CO_2 molecules are absorbed through the interface leading to the depletion of the hydroxyl ions thus and increasing the concentration carbonate ions vial Eqs. (3.8) and (3.9). Going by the Le Chatelier's principle, an increase in carbonate ions favors the reverse of reaction in Eq. (3.9), leading to a favorable forward reaction in Eq. 3.8 (Yoo *et al.*, 2012). The net effect is a decrease in concentration of bicarbonate ions and the pH of the solution. The overall absorption process is then represented by Eq. (3.11).



At equilibrium, an increase in CO_2 may be absorbed to make up for the shortage of physically unabsorbed CO_2 in water during the reaction (Yoo *et al.*, 2012). If aq $NaOH$ solution is the limiting reactant, absorption of CO_2 is summarized by Eq. 3.12, which is the net reaction of Eq. 3.10 and 3.11.



3.2.3. The reaction rate constant

For the elementary reaction, represented by Eq. 3.10, assuming constant temperature, the rate of reaction remains constant and any change in the reactivity is attributed to change in the activity of the reacting species (Stolaroff *et al.*, 2008). This reaction is represented by a rate constant k_{OH^-} , and is a relatively fast reaction, enhancing mass transfer of CO_2 molecules across the interface. This rate depends on the availability of counter ions (α^+) and is limited to low temperatures with values showing diversity and scattering especially for a second-order rate constant (Gondal, 2014). To accommodate high solvent

concentration and the non-ideality behavior of a system caused by the scattering. The function is modified by introducing the ionic strength of the active species in the system to counter the non-idealities in the kinetic constant, resulting in the following expression for the reaction rate constant (Haubrock *et al.*, 2005).

$$k_{OH,\alpha^+} = k_{OH^-}^{\infty}(T) \times 10^{(a \cdot I^2 + b \cdot I)} \quad (3.15)$$

Where $k_{OH^-}^{\infty}$ is the reaction rate constant at infinite dilution which has previously been evaluated to be $5881 \text{ m}^3/\text{kmol} \cdot \text{s}$ (Pohorecki and Moniuk 1988). I is the solution's ionic strength which, in a 1:1 electrolyte, and each singly charged ion equals the concentration of the solvent. It is calculated using Eq. 3.16 (Dragan, S., 2016).

$$I = 0.5 \left(\sum [CO_2]^i Z_i^2 \right) = C_x \quad (3.16)$$

The second-order reaction rate constant is thus given as;

$$\begin{aligned} k_{C_x, Na^+} &= k_{C_x}^{\infty} \left(10^{(0.1987 C_x - 0.012 (C_x)^2)} \right) \\ &= 5881 \left(10^{(0.1987 C_x - 0.012 (C_x)^2)} \right) \end{aligned} \quad (3.17)$$

The reflection of the experimental results is more enhanced in derived expressions incorporating the activity of the species than the ones based on the concentration of the reacting species alone and is more applicable to highly non-ideal systems, where both polar and non-polar components are involved (Haubrock *et al.*, 2005).

3.2.4. Henry's law constant

The Henry's law constant (H^{cp}) is a representation of the solubility of the solute in the liquid phase and is estimated by Eq. 3.18.

$$\lg \left(\frac{H^{cp}}{H_{H_2O}^{cp}} \right) = -K_s(I) \quad (3.18)$$

where K_s is the summation of the ion coefficients in the system.

$$K_s = (i_- + i_+ + i_g) = (i_{Na^+} + i_{OH^-} + i_{CO_3^{2-}} + i_{CO_2}) \quad (3.18)$$

For the system $CO_2/NaOH/H_2O$ the values of the coefficients are according those used by (Danckwerts, 1970);

$$i_{Na^+} = 0.091, \quad i_{OH^-} = 0.066, \quad i_{CO_3^{2-}} = 0.021, \quad i_{CO_2} = -0.019 \quad (3.19)$$

This gives 0.159 as the value of K_s

$$\lg\left(\frac{H^{cp}}{H_{H_2O}^{cp}}\right) = -K_s(I) = -0.159(I) \quad (3.20)$$

This constant is a function of the ionic strength I , and the reaction temperature T (Pohorecki and Moniuk, 1988) and for a purely physical absorption, the constant is exclusively a function of the operating temperature and is calculated using Eq. 3.21 (Dragan, 2016).

$$\lg(H_{H_2O}^{cp}) = \left(\left(\frac{1140}{T}\right) - 5.30\right) \quad (3.21)$$

where T is the temperature in Kelvins

At $T = 298K$,

$$\lg(H^{cp})^0 = \left(\frac{1140}{298}\right) - 5.30 = -1.4744 \quad (3.22)$$

$$(H^{cp})^0 = 0.0331 \text{ mol/m}^3 \cdot \text{Pa} \quad (3.23)$$

The ionic strength I is calculated using Eq. 3.16 and the transformed equation is given in Eq. 3.24.

$$H^{cp} = 0.0335\{10^{(-0.159c_x)}\} \quad (3.24)$$

3.3. Mass transfer models

3.3.1. The two film theory

In quantifying CO_2 absorption in a packed column, the widely used fundamental mass transfer model is the two film model. This model, proposed by Whitman in 1923, is the simplest theory designed for the analysis of mass transfer between phases (Maheswari *et al.*, 2014). The model assumes that there exists a gas and liquid film of equal thickness on either side of the interface between the phases where all the resistance to mass transfer is localized (Nair and Selvi, 2014). A schematic representation of the two films is presented in Figure 1.

Due to the absence of turbulence in the two films, flow is assumed to be laminar and the transfer of CO_2 is exclusively by molecular diffusion. The transfer experience a series of resistance in the two films that sum up to the overall resistance (Kumar *et al.*, 2012; Wang *et al.*, 2012; Pinto *et al.*, 2016).

3.3.1.1. Films resistances in physical absorption

The films resistances in an heterogeneous is used to model the coefficient of CO_2 transfer across the interface (Shafeeyan *et al.*, 2014). This coefficient is an important parameter used in the design and operation of process equipment and is estimated with minimum error using theoretical equations, film

correlations and analogies that are functions of the properties of both gas and liquid phases and the fluid flow within the column.

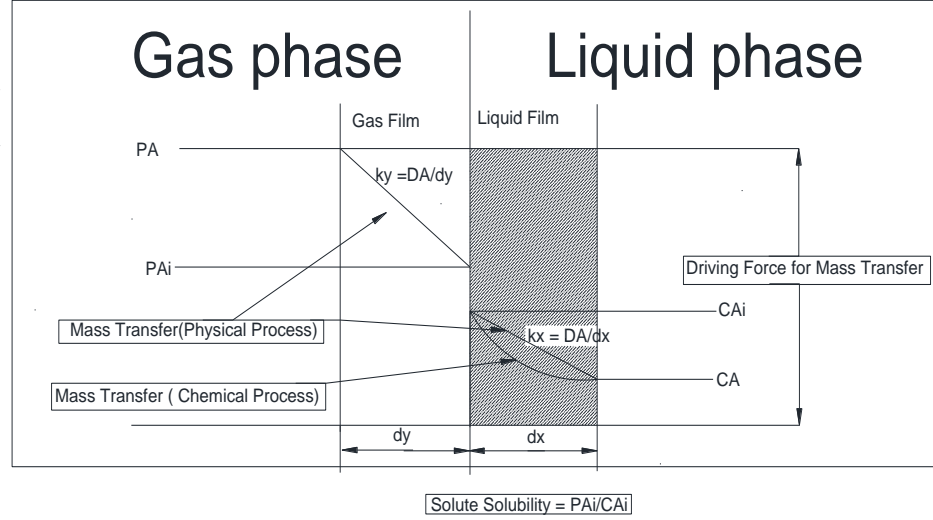


Figure 3. 1: Schematic representation of the two film at the interface between the phases.

In both physical and chemical absorption, a dynamic rate of diffusion of CO_2 molecules is observed in the early stages of the processes, however, as time lapses, a steady rate of diffusion is attained leading to an equalized mass flux within the films (Shafeeyan *et al.*, 2014). This flux is expressed as defined in the Fick's law of diffusion. In the liquid film, the flux is given by Eq. 3.25

$$N_{CO_2} = -D_{CO_2,x} \frac{dC_{CO_2}}{dz} \quad (3.25)$$

Where $D_{CO_2,x}$ is CO_2 diffusivity in in the liquid phase and C_{CO_2} is CO_2 concentration in the film. In this film, concentration is expressed in terms of CO_2 partial pressures. Assuming the gas obeys the ideal gas law.

$$C_{CO_2} = \frac{n_{CO_2}}{v} = \frac{P_{CO_2}}{RT} \quad (3.26)$$

Thus the flux in the gas phase is derive by substituting equation 3.26 into equation 3.25,

$$N_{CO_2} = \left(\frac{-D_{CO_2}}{RT} \right) \frac{dP_{CO_2}}{dz} \quad (3.27)$$

Integrating the flux over the distance Z ,

$$N_{CO_2} \int_0^Z dz = - \left(\frac{D_{CO_2}}{RT} \right) \int_{P_{CO_2}}^{P_{CO_2}^i} dP_{CO_2} \quad (3.28)$$

$$N_{CO_2} = \left(\frac{-D_{CO_2}}{RTZ} \right) (P_{CO_2} - P_{CO_2}^i) \quad (3.29)$$

Here, z represents the respective gas and liquid film thickness, y and x respectively and $P_{CO_2}^i$ is CO_2 concentration at the interface.

In this equation, two parameters are difficult to quantify. One is the thickness of the films which are not readily available as the discontinuity of the CO_2 concentration between the interface and the bulk of the liquid cannot be established with any measure of certainty (Song, 2017). To circumvent this Eq. 3.29 is expressed using mass transfer coefficients.

$$N_{CO_2} = k_y (P_{CO_2} - P_{CO_2}^i) \quad (3.30)$$

Where k_y is the gas film mass transfer coefficient given Eq. 3.31;

$$k_y = \frac{-D_{CO_2}}{RTy} \quad (3.31)$$

Similarly, for the liquid film:

$$N_{CO_2} = k_x (C_{CO_2}^i - C_{CO_2}) \quad (3.32)$$

Where, k_x is the liquid film mass transfer coefficient. These coefficients largely depend on the experimental conditions (Whitman, W. G., 1923). Therefore, the flux can also be expressed as a function of the overall mass transfer coefficient based on the gas and liquid films by Eq. 3.33.

$$N_{CO_2} = K_y (P_{CO_2}^* - P_{CO_2}) = K_x (C_{CO_2} - C_{CO_2}^*) \quad (3.33)$$

Where, $P_{CO_2}^*$ is CO_2 partial pressure that is in equilibrium with CO_2 concentration in the liquid phase i.e. C_{CO_2} , while $C_{CO_2}^*$ is CO_2 concentration in the liquid phase that is in equilibrium with the partial pressure in the gas phase i.e. P_{CO_2} . K_y and K_x are the overall mass transfer coefficients based on the gas and liquid phase concentrations respectively. Another difficulty is determining the interface concentrations $P_{CO_2}^i$ and $C_{CO_2}^i$. Having assumed the existence of equilibrium at the interface, and going by the Henry's law, it follows that the following relationship holds (Mustafa *et al.*, 2020).

$$P_{CO_2}^i = H^{cp} C_{CO_2}^i \quad (3.34)$$

Where H^{cp} is the Henry's law constant for the system in $kmol/m^3 \cdot atm$, used to predict the physical solubility of the CO_2 in the solvent (Mustafa *et al.*, 2020).

Since the concentrations at the interface cannot be measured, the individual coefficients of the films are defined based on the difference in the bulk concentration in one phase and the concentration that would be in equilibrium with it the other phase. A distribution factor is then used to unify the driving force across the phases (Song, 2017).

$$P_{CO_2}^* = H^{cp} C_{CO_2} \quad (3.35)$$

$$C_{CO_2}^* = H^{cp} P_{CO_2} \quad (3.36)$$

The gas phase overall flux equation is then expanded to include the concentration at the interface.

$$N_{CO_2} = K_y (P_{CO_2}^* - P_{CO_2}) \quad (3.37)$$

$$= K_y \{ (P_{CO_2}^* - P_{CO_2}^i) + (P_{CO_2}^i - P_{CO_2}) \} \quad (3.38)$$

From Eqs. 3.30, 3.32, 3.34 and 3.35, Eq. 3.38 can then be written as;

$$N_{CO_2} = K_y \{ H^{cp} (C_{CO_2} - C_{CO_2}^i) + (P_{CO_2}^i - P_{CO_2}) \} \quad (3.39)$$

$$= K_y \left\{ H_{cp} \left(\frac{N_{CO_2}}{k_x} \right) + \left(\frac{N_{CO_2}}{k_y} \right) \right\} \quad (3.40)$$

$$\frac{1}{K_y} = \frac{1}{k_y} + \frac{H_{cp}}{k_x} \quad (3.41)$$

This is the equation for the overall resistance based on CO_2 concentration in the gas phase and is a summation of the resistances in both the gas and liquid films (Hegely *et al.*, 2017). A similar equation can be derived based on CO_2 concentration in the solvent.

$$\frac{1}{K_x} = \frac{1}{H^{cp} k_y} + \frac{1}{k_x} \quad (3.42)$$

3.3.1.2. Films resistances in chemisorption processes

In chemisorption, absorption of CO_2 aided by the reaction between CO_2 molecules and the solvent. Astarita and Danckwerts have extensively studied this subject in systems with varied reaction rates, from

very slow to instantaneous reactions, and they concluded that the reaction enhances mass transfer of CO_2 molecules by a factor known as the enhancement factor β . This is the ratio of transfer coefficient in a chemisorption process to that of a purely physical absorption as expressed in Eq. 3.43 (Astarita *et al.*, 1983; Oinas *et al.*, 1995 Kimweri, 2001).

$$\beta = \frac{k_x}{k_x^0} \quad (3.43)$$

Where β is the enhancement factor,

k_x is the liquid film's mass transfer coefficient for chemisorption,

k_x^0 is the film's mass transfer coefficient for a physical absorption.

In a first or a pseudo first order reaction, β is expressed in terms of Hatta number (Ha) in Eq. 3.44.

$$\beta = \frac{1}{C_{CO_2}^*} \left(C_{CO_2}^* - \frac{C_{CO_2}^\infty}{\cosh(Ha)} \right) \frac{Ha}{\tanh(Ha)} \quad (3.44)$$

where $C_{CO_2}^*$ is CO_2 concentration in equilibrium with the concentration in the gas phase,

$C_{CO_2}^\infty$ is CO_2 concentration in the bulk of the liquid phase,

Ha is the Hatta number for the system.

The Hatta number is defined by.

$$Ha = \frac{\sqrt{k_2 D_{CO_2} \cdot C_{CO_2}^\infty}}{k_x} \quad (3.45)$$

Where k_2 is the second order reaction rate constant.

The approximation of β was done by Danckwerts for the case where the bulk concentration of CO_2 in the liquid phase $C_{CO_2}^\infty$, is non-existent and the relationship between the two parameters is given by the following equation (Garcia *et al.*, 2018):

$$\beta = \sqrt{1 + (Ha)^2} \quad (3.46)$$

This holds for $Ha > 3$ and for reaction of the first order regime with $2 < Ha < \beta^\infty$, with β equalling Ha for a pseudo-first order reaction (Nathalie *et al.*, 2012; Pinto *et al.*, 2016).

$$\beta = Ha \quad (3.47)$$

Based on CO_2 concentration in the gas phase, the flux in a chemisorption process is expressed as;

$$N_{CO_2} = K_y \left\{ H^{cp} \left(\frac{N_{CO_2}}{\beta k_x^o} \right) + \left(\frac{N_{CO_2}}{k_y} \right) \right\} \quad (3.48)$$

Where N_{CO_2} is CO_2 flux across the interface,

K_y is the overall mass transfer coefficient based on the gas film's coefficient,

H^{cp} is the Henry's law constant.

The overall resistance is expressed by Eq. 3.50;

$$\frac{1}{K_y} = \frac{1}{k_y} + \frac{H^{cp}}{\beta k_x^o} \quad (3.50)$$

And for the CO_2 concentration in the liquid phase,

$$\frac{1}{K_x} = \frac{1}{H^{cp} k_y} + \frac{1}{\beta k_x^o} \quad (3.51)$$

Where K_x is the overall mass transfer coefficient based on the liquid film's coefficient.

A fast-order or a pseudo-first-order reactions with large β has been found to create minimal resistance in the liquid film and the rate of absorption is controlled by the diffusion across the gas film.

This then becomes the limiting factor for mass transfer (Whitman, 1923).

3.3.2. The Effective mass transfer area

For a system with a pseudo first-order reaction in the liquid film where the process is controlled by the chemical reaction in the liquid film, the apparent gas film mass transfer coefficient (k'_y) is described by Eq. 3.52.

$$k'_y = \frac{\sqrt{k_{C_x} \cdot C_x \cdot D_{CO_2 \cdot x}}}{H^{cp}} \quad (3.52)$$

Using CO_2 mole fraction of the gas to and from the column y_a and y_b respectively, the effective area (a_e), is calculated using Eq. 3.53 (Wang *et al.*, 2012).

$$a_e = \frac{u_y}{K_y ZRT} \cdot \ln\left(\frac{y_a}{y_b}\right) \approx \frac{u_y}{k'_y ZRT} \cdot \ln\left(\frac{y_a}{y_b}\right) \quad (3.53)$$

Where;

k_{OH^-} is the second order reaction rate constant, ($m^3/kmol \cdot s$),

C_x is the concentration of free hydroxyl ion in the liquid phase, ($gmol/L$),

$D_{CO_2 \cdot x}$ is the diffusivity of the solute in the liquid phase, (m^2/s),

H^{cp} is the Henry's constant for the solute, ($kmol \cdot m^{-3} \cdot Pa$),

y_a and y_b are the respective CO_2 mole fractions of the gas to and from the column,

Z is the height of the packed bed, (m).

This is a convenient method for evaluating a_e , as the only measurement to be made are the solvent concentration and the solute concentration in the column's inlet and outlet gas streams.

3.3.3. The overall mass transfer coefficient

The overall coefficient is the reciprocal of the overall resistance to the absorption process.

$$K_y = \left(\frac{1}{k_y} + \frac{H^{cp}}{\beta k_x^o} \right)^{-1} \quad (3.54)$$

For a fast reaction, β is bound to be large, a phenomena created by an increase in hydroxide ions in the liquid bulk justifying the treatment of the reaction as a pseudo-first-order reaction. Experiments done on wetted wall columns have shown that liquid film resistance accounts for less than 10% of the overall mass transfer coefficient (Wang *et al.*, 2012). An assumption is that the overall coefficient is equal to the coefficient in the liquid film.

$$K_y a_e = \frac{u_y}{ZRT} \cdot \ln \left(\frac{y_a}{y_b} \right) \quad (3.55a)$$

Where

$$K_y = \frac{\beta k_x^o}{H^{cp}} = \frac{\sqrt{k_2 D_{CO_2} x C_{CO_2}^\infty}}{H^{cp}} \quad (3.55b)$$

3.4. Process optimization

In science and engineering optimization of a process involves experiments in which input variables are changed according to a given rule in order to identify the reasons for the change in the output response parameter (Cavazzuti, 2015). It has found popularity in design, construction and maintenance systems where engineers and scientists make many technological and managerial decision to arrive at a desired output. The decision made may either be to minimize or maximize the quantity of the input parameters or a combination of both. A number of optimization methods have been developed and applied to various optimization processes. They are the Randomized complete block design, the Latin square, full and fractional factorial, Box-Behnken, and Plackett-Burman among others. This thesis considers a design of experiment (DOE) called the Taguchi method of optimization.

3.4.1. The Taguchi philosophy

In a full factorial method of optimization involving different parameters, the different combination of the factors and the levels are investigated which is, time consuming and costly. To overcome this, Taguchi method of optimization is used (Qafery *et al.*, 2018). The method was developed by a Japanese quality engineer called Dr. Genichi Taguchi who in the 1950s while working in Japanese industries stressed the importance of quality improvement in products and/or processes by the use of statistical experimental design that can easily be adopted by designers with limited knowledge of statistics, enticing

scientists and engineers alike (Sekulić, *et al.*, 2011; Cavazzuti, 2015; Pragajibhai *et al.*, 2018; Yang *et al.*, 2020). The method applies a system of arrays that allows orthogonal estimation of the minimum number of experimental runs, resulting in reduction in production time with a decrease in cost while improving profitability (Sudhakara and Parvathi, 2014; Dwivendi and Das, 2015; Qafery *et al.*, 2018).

Although the Taguchi philosophy has far reaching consequences, three concepts are considered to be its foundation (Davis and John, 2018):

- 1) Quality should be designed into the product and not inspected into it,
- 2) Quality is better achieved by minimizing the deviation from the target and that the product should be designed that it is immune to uncontrollable environmental factors,
- 3) The cost quality should be measured as a function of deviation from the standard and the losses should be measured system-wide.

3.4.2. Experimental planning

3.4.2.1. The design of experiments

The Taguchi method is one among many DOEs that systematically apply statistics to experimentation and guides the choice of experiment to be performed in an efficient way with the objective of optimizing the process (Sudhakara and Prasanthi, 2014; Qafery *et al.*, 2018; Davis and John, 2018). A sequence of tests is designed where the input (experimental factors) and its effect on the output registered to find the desired optimal settings. It is a quick and cost effective tool used in optimization of products and/or processes (Davis and John, 2018).

There is an array of DOE techniques that a designer of an experiment can chose from but there is no “best choice” among the options available. The correct technique of selection depends on the intended investigation and the aim of the experiment. When deciding on the technique, the items to be considered are as follows (Davis and John, 2018):

- 1) The number of experiments (n) that can be carried out cost effectively and within the time constrains,
- 2) The number of factors (k), of the experiment. As the number of factors increases, the number of experimental runs required increases exponentially in many DOE techniques.

In order to reduce the size and laboriousness of the problem, the general rule is to reduce the number of factors considered (Dave and John, 2018).

3.4.2.2. Selection of the Orthogonal Array

This is a special design method used to reduce the number of experiments to be carried out which opens the way for more factors to be considered. The selection of the Orthogonal Array (OA), is guided by the computational degree of freedom (DOF), which is an important number in statistical analysis and is normally one less than the number of experiments (Muhammad *et al.*, 2012; Qafery *et al.*, 2018; Davis and John, 2018). In the presence of interaction between the factors, DOF becomes the product of the number of DOFs of the main effects involved in the interaction (Kukreja *et al.*, 2011). For any given factor;

$$DOF = \text{number of levels} - 1 \quad (3.56)$$

3.4.2.3. Quality loss function

In the Taguchi method, quantification of response parameter achieved by the quality loss function. It is a continuous function defined as the deviation of the values of the response parameter from the ideal value. It is commonly referred to as the mean square deviation (MSD). This function is transformed into the signal-to-noise ratio ψ , by the following mathematical computation (Sekulić, *et al.*, 2011; Muhammad *et al.*, 2012; Davis and John, 2018).

$$S/N = \psi = -10 \log\{MSD\} \quad (3.57)$$

The quality characteristics of the response parameter are grouped in three categories of ψ , namely “the smaller-the-better”, “the normal-the-better” and “the larger-the-better” and their computations are represented in table 3.1 (Muhammad *et al.*, 2012; Davis and John, 2018).

Table 3. 1: Types of problems and the respective signal-to-noise ratio.

Choose...	ψ formulas	Use when the goal is to
Smaller-the-better	$\psi = -10 \log \left[\frac{1}{n} \sum_{i=1}^n y_i^2 \right]$	Minimize the response
Normal-the-better	$\psi = 10 \log \left(\frac{\mu^2}{\sigma^2} \right)$	Target the response and you want to base the S/N ratio on means and standard deviation
Larger-the-better	$\psi = -10 \log \left[\frac{1}{n} \sum_{i=1}^n \left(\frac{1}{y_i^2} \right) \right]$	Maximize the response parameter

Where n is the number of trials,

y_i is the mean,

σ the standard deviation of the observed data at the i^{th} trial.

The desired ψ , is an inverse of variance, chosen after performing the experiments as per the chosen array. The function is used to minimize variability during optimization of a product or the process with the reduced variability of the product and/or the process against undesirable changes in noise factors is realized if and only if ψ is maximized so that the factors chosen produce maximum values of ψ as the ratio and variance are inversely proportional. A single overall value of ψ for all the quantity characteristics can be performed for all the quantity in a multi-objective optimization with the new ratio being the MSNR. The MSNR for the j^{th} trial is computed by Eq. 3.58.

$$(MSNR)_j = -10 \log_{10} \left(\sum_{i=1}^n (w_i, y_{ij}) \right) \quad (3.58)$$

with

$$y_{ij} = \frac{L_{ij}}{L_{i^*}} \quad (3.59)$$

Where;

Y_j is the total normalized quality loss in j^{th} trial,

w_i represents the weighting factor for the i^{th} quality characteristics,

k is the normalized quality loss associated with the i^{th} quality characteristic at the j^{th} trial condition which varies from a minimum of zero to a maximum of 1,

L_{ij} is the quality loss or MSD for the i^{th} quality characteristic at the j^{th} trial

L_{i^*} is the maximum quality loss for the i^{th} quality characteristic among all the experimental runs (Muhammad *et al.*, 2012).

3.4.3. Steps in optimization process

The following is the sequence of events in the process of optimization using the Taguchi method (Davis and John, 2018):

- Step 1: Identify the response parameter and the objective
- Step 2: Identify process variables, that act as the experimental factors, and their levels,
- Step 3: Determine the suitable orthogonal array (OA),
- Step 4: Assign factors and interactions to the column of the array.
- Step 5: Conduct the experiments.

Step 6: Calculate the signal-to noise ratio ψ , and determine the optimum setting of the factor levels.

Step 7: Perform confirmatory experiment.

3.4.4. ANOVA and its significance

The analysis of variance (ANOVA) is a statistical method developed by Ronald Fisher in 1918. It is an extended version of the T -test and the Z -test, used to model the relative significance of individual factors on the response parameter when the individual factors are evaluated at two or more levels (Muhammad *et al.*, 2012; Sudhakara and Prasanthi, 2014; Davis and John, 2018). In this method, the total sum of squares deviation (SS_T) for all the runs is evaluated using Eq. 3.60.

$$SS_T = \sum_{i=1}^n y_i^2 - CF \quad (3.60)$$

with

$$CF = \frac{T^2}{n} \quad (3.61)$$

where;

n is the total number of experiments in the orthogonal array,

y_i is the response parameter in the i^{th} experiment

CF is the correction factor calculated using Eq. 3.61.

T is the totals of the response parameter, and n is the product of the number of trials and the number of repetitions.

The sum of squares deviation of each of the factors calculated using Eq. 3.62.

$$SS_f = \{(A_1^2/N_{f1}) + (A_2^2/N_{f2}) + \dots + (A_n^2/N_{fn})\} - CF \quad (3.62)$$

Where, A_i is the sum of the squares of the response parameter at level i where the factor A contributes,

N is the number of response parameters in that level and n is the number of levels.

The variance V , of any factor is the ratio of the factors sum of squared response to its degree of freedom (DOF_f).

$$V_f = \left(\frac{SS_f}{DOF_f} \right) \quad (3.63)$$

Variance ratio F , is the ratio variance of a factor to that of the residue;

$$F_f = \frac{V_f}{V_e} \quad (3.64)$$

Statistically, this is the F –test, used to investigate the significance of each factor and/or interactions thereof on the response parameter (Penteado *et al.*, 2016). If $F > 4$, any change in the magnitude of the factor posts a significant effect on the response parameter and the greater the value of F_f , the more the influence on the response parameter (Kamaruddin *et al.*, 2004; Muhammad *et al.*, 2012).

The percentage contribution of a factor (P_i) is the ratio of the sum of squares of a factor to that of the total result expressed as a percentage

$$P_f = \left(\frac{SS_f}{SS_T} \right) \times 100\% \quad (3.65)$$

3.5. Mathematical modelling

3.5.1. An overview

Differential equations play an important role in modelling natural phenomena and finds application in biomathematics, economics, finance, science and engineering. In this study, differential equations would give more insight in the study of absorption of CO₂ in a packed column (Mondal *et al.*, 2015). The equation may either be an ordinary differential equation (ODE) or a partial differential equation depending on the number of variable considered in the when modelling the subject at hand. These models can either be solved analytically using techniques like the separation, Laplace transforms, Fourier transforms for an exact solution or solved using numerically for an approximate solution, assuming the presence of stage wise elements in the computational domain (Ω), where continuum conditions are maintained (Kenig & Seferlis, 2015).

In the domain, mass transfer of CO₂ molecules from the gas phase to the liquid phase is ascribed by diffusion, convection and the reaction between the CO₂ and the solvent (Kim A.S., 2020). A formulation of a comprehensive model considers the effects of column hydrodynamics, diffusivity of solutes and solvent molecules and chemical kinetics driving the reaction in the liquid film. Depending of the objective of the analysis, the model may be used to describe either the transient or steady state CO₂ concentration profile in the packed section of the column for industrial and laboratory scale reactors (Gheni *et al.*, 2018).

3.5.2. Model development

The bed (the computational domain ψ , is divided into N differential volumes (elements) as represented in Figure 3.2 and based on conservation principles, a model is constructed on each of the elements, augmented by appropriate rate of reaction between the reactants, together with diffusion of CO_2 molecules across the interface (Shafeeyan *et al.*, 2014).

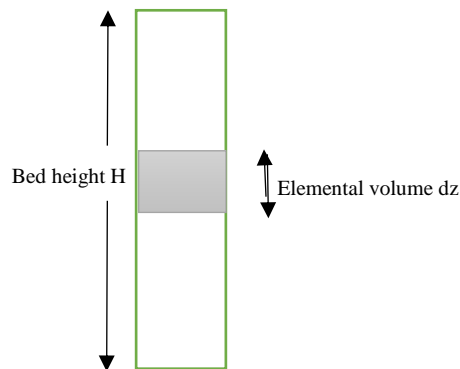


Figure 3. 2: Schematic representation of the elements in the computational domain.

It is assumed that:

- i. Transfer of CO_2 molecules is exclusively by diffusion,
- ii. The gas phase is a binary mixture of CO_2 and CH_4
- iii. Mass transfer is unidirectional, from the gas phase to the liquid phase
- iv. Only the axial diffusion prevails with no radial diffusion,
- v. The reaction taking place is a pseudo-first order reaction,
- vi. Isothermal conditions are maintained in the bed,
- vii. The solvent is in excess of CO_2 and its concentration is remains constant along the bed,
- viii. The two phases maintain a steady plug flow in the bed,
- ix. There is a negligible pressure drop in the bed,
- x. The solvent is non-volatile at the cooperating conditions,
- xi. CO_2 solubility in the solvent obeys Henry's law of solubility.

At the transition time, normally experienced during start-up and shut down, the profile is best described using two PDEs, one for the gas phase and the other for the liquid phase, and are generated for each element in the domain. Since there is an assumption that the solvent is in excess of the solute, the solvent concentration in the liquid phase is assumed to remain constant in the domain and in that regard, the gas phase PDE is considered in the model.

In the element, the sum of molecules entering the column and those generated is equal to the sum of these leaving, accumulating and those being consumed by the reaction. This mass balance is represented in Eq. 3.66

$$\begin{aligned} & \text{amount of } CO_2 \text{ entering} + \text{ammount of } CO_2 \text{ generated} \\ & = \text{amount of } CO_2 \text{ leaving} + \text{amount of } CO_2 \text{ accumulating} \\ & + \text{amount of } CO_2 \text{ reacting} \end{aligned} \quad (3.66)$$

This computation is performed in each element in the domain.

At the entry to the first element, movement of CO_2 molecules is influenced by convection and diffusion forces, respectively presented by Eqs. 3.67 and 3.68.

$$uC_{CO_2}S \quad (3.67)$$

$$-D_{CO_2} \frac{dC_{CO_2}}{dz} S \quad (3.68)$$

The same phenomena occur at the last element in the domain where the convection and diffusion are presented by Eqs. 3.69 and 3.70 respectively.

$$u \left(C_{CO_2} + \frac{dC_{CO_2}}{dz} \right) S \quad (3.69)$$

$$-D_{CO_2} \left(\frac{dC_{CO_2}}{dz} + \frac{d}{dz} \left(\frac{dC_{CO_2}}{dz} \right) dz \right) S \quad (3.70)$$

The amount of molecules accumulating and reacting within an element is expressed by Eqs. 3.71 and 3.72.

$$\frac{dC_{CO_2}}{dt} S dz \quad (3.71)$$

$$r_{CO_2} = (-k_2 C_{CO_2} C_{NaOH}) \quad (3.72)$$

Any other source or sink is represented by F

Assuming the gas phase obeys the ideal gas law, the CO_2 concentration is assumed to be a function of the initial concentration and its mole fraction as represented in Eq. 3.73

$$C_{CO_2} = \left(\frac{P}{RT} \right) C_{CO_2o} y_{CO_2} \quad (3.73)$$

Where y_{CO_2} is the solute mole fraction in the gas phase. On differentiating;

$$\frac{dC_{CO_2}}{dz} = \left(\frac{P}{RT} \right) C_{CO_2o} \frac{dy_{CO_2}}{dz} \quad (3.74)$$

and

$$\frac{d^2 C_{CO_2}}{dz^2} = \left(\frac{P}{RT}\right) C_{CO_2 O} \frac{d^2 y_{CO_2}}{dz^2} \quad (3.75)$$

The rate of reaction is a function of the concentration of the reacting species

$$r_{CO_2} = k \left(\frac{P}{RT}\right) C_{CO_2 O} y_{CO_2} C_{NaOH} \quad (3.76)$$

With no generation in the differential volume, the solute balance over the differential volume reduces to:

$$\text{Input rate} = \text{Output rate} + \text{Consumption} + \text{Accumulation}$$

$$\begin{aligned} C_{CO_2 O} \frac{\partial y_{CO_2}}{\partial t} S dz &= u C_{CO_2 O} y_{CO_2} S - D_{CO_2} C_{CO_2 O} \frac{\partial y_{CO_2}}{\partial z} S dz - u C_{CO_2 O} \left(y_{CO_2} + \frac{\partial y_{CO_2}}{\partial z} dz \right) S dz \\ &+ D_{CO_2} C_{CO_2 O} \left(\frac{\partial y_{CO_2}}{\partial z} + \frac{\partial}{\partial z} \left(\frac{\partial y_{CO_2}}{\partial z} \right) dz \right) S \\ &- C_{CO_2 O} \{ (-k_2 y_{CO_2} C_x) + \mathbf{F} \} S dz \end{aligned} \quad (3.77)$$

Dividing through by $C_{CO_2 O} S dz$ and assuming that the reactant are consumed exclusively by the reaction,

$$\frac{\partial y_{CO_2}}{\partial t} = -u \left(\frac{\partial y_{CO_2}}{\partial z} \right) + D_{CO_2} \left(\frac{\partial^2 y_{CO_2}}{\partial z^2} \right) - k_1 y_{CO_2} \quad (3.78)$$

Where $k_1 = k_2 C_x$

This is a transient convection-diffusion-reaction (CDR) equation that provides CO_2 concentration in the domain and is solved with the aid of appropriate boundary conditions (Pradeep, 2010).

Table 6.1: Boundary conditions and ODEs for an absorption column with radial dispersion (Adopted from Pradeep, 2010).

ODEs for plug flow reactor	Boundary condition at $z = 0$	Boundary condition At $z = L$
$D_{CO_2} \frac{d^2 C_A}{dz^2} - u \frac{dC_A}{dz} - k_1 C_A = 0$	$u C_{A(in)} = u C_A - D_{CO_2} \frac{dC_A}{dz}$	$\frac{dC_A}{dz} = 0$
$D_{CO_2} \frac{d^2 C_B}{dz^2} - u \frac{dC_B}{dz} + k_1 C_A = 0$	$u C_{B(in)} = u C_B - D_{CO_2} \frac{dC_B}{dz}$	$\frac{dC_B}{dz} = 0$

The boundary conditions as proposed by Danckwerts are (Pradeep, 2010);

- i. At the gas inlet i.e. $x = 0$, the presence of dispersion inside in the bed modifies the flux of the entering gas stream, $u y_{CO_2(in)}$ to $u y_{CO_2} - D_{CO_2} \frac{dy_{CO_2}}{dz}$

$$uy_{CO_2(in)} = uy_{CO_2} - D_{CO_2} \frac{dy_{CO_2}}{dz} \quad (3.79)$$

ii. At the outlet, i.e. $x = 1$, the rate of change of the solvent concentration is assumed to be zero.

$$\frac{dy_{CO_2}}{dz} = 0 \quad (3.80)$$

3.5.3. Solution of the CDR equation

Discretization of the CDR is done for the individual terms in the equation. The diffusion term is discretized using the central difference scheme while the convective term is discretized using the upwind difference scheme as in Eq. 3.81.

$$D_{CO_2} \left(\frac{y_{CO_2(i+1)} + y_{CO_2(i-1)} - 2y_{CO_2(i)}}{\Delta Z^2} \right) - u \left(\frac{y_{CO_2(i)} - y_{CO_2(i-1)}}{\Delta Z} \right) - k_1 y_{CO_2(i)} = 0 \quad (3.81)$$

All the other sources and sinks are assumed to be non-existent i.e. $F = 0$.

The discretization done at all the nodes in Ω that are placed at the points joining the elements, and at the entrance and exit (Pradeep, 2010).

At node 1, which is the node at the bottom of the bed, the discretized equation is given by Eq. 3.82.

1) At node 1

$$D_{CO_2} \left(\frac{y_{CO_2(2)} + y_{CO_2(0)} - 2y_{CO_2(1)}}{\Delta Z^2} \right) - u \left(\frac{y_{CO_2(1)} - y_{CO_2(0)}}{\Delta Z} \right) - k_1 y_{CO_2(1)} = 0 \quad (3.82)$$

On re-arranging;

$$y_{CO_2(1)} \left(-\frac{D_{CO_2}}{\Delta Z^2} - \frac{u}{\Delta Z} - k_1 \right) + y_{CO_2(2)} \left(\frac{D_{CO_2}}{\Delta Z^2} \right) + y_{CO_2(0)} \left(\frac{D_{CO_2}}{\Delta Z^2} - \frac{u}{\Delta Z} \right) = 0 \quad (3.83)$$

The first boundary condition is given by Eq. 3.84.

$$uy_{CO_2(in)} = uy_{CO_2(1)} - D_{CO_2} \left(\frac{y_{CO_2(2)} - y_{CO_2(0)}}{2\Delta Z} \right) \quad (3.84)$$

Solving for $y_{CO_2(0)}$

$$y_{CO_2(0)} = \frac{2\Delta Z}{D_{CO_2}} (y_{CO_2(in)} - y_{CO_2(1)}) - y_{CO_2(2)} \quad (3.85)$$

$y_{A(0)}$ is then substituted in Eq. 3.86

$$y_{CO_2(1)} \left(-\frac{2D_{CO_2}}{\Delta Z^2} - \frac{u}{\Delta Z} - k_1 \right)$$

$$+y_{CO_2(2)} \left(\frac{D_{CO_2}}{\Delta Z^2} \right) + \left(\frac{2u\Delta Z}{D_A} \right) \left(\frac{D_{CO_2}}{\Delta Z^2} - \frac{u}{\Delta Z} \right) (y_{CO_2(in)} - y_{CO_2(1)}) = 0 \quad (3.86)$$

$$\begin{aligned} \left(-\frac{2D_{CO_2}}{\Delta Z^2} - \frac{3u}{\Delta Z} - \frac{2u^2}{D_{CO_2}} - k_1 \right) y_{CO_2(1)} + \left(\frac{2D_{CO_2}}{\Delta Z^2} + \frac{u}{\Delta Z} \right) y_{CO_2(2)} \\ = -\left(\frac{2u^2}{D_{CO_2}} + \frac{2u}{D_{CO_2}} \right) y_{CO_2(in)} \end{aligned} \quad (3.87)$$

At node 2;

$$\left(\frac{D_{CO_2}}{\Delta Z^2} + \frac{u}{\Delta Z} \right) y_{CO_2(1)} + \left(-\frac{2D_{CO_2}}{\Delta Z^2} - \frac{u}{\Delta Z} - k_1 \right) y_{CO_2(2)} + \left(\frac{2u^2}{D_{CO_2}} \right) y_{CO_2(3)} = 0 \quad (3.88)$$

This is replicated at all the subsequent nodes in the domain up to node $n - 1$,

$$\left(\frac{D_{CO_2}}{\Delta Z^2} + \frac{u}{\Delta Z} \right) y_{CO_2(n-2)} + \left(-\frac{2D_{CO_2}}{\Delta Z^2} - \frac{u}{\Delta Z} - k_1 \right) y_{CO_2(n-1)} + \left(\frac{2u^2}{D_{CO_2}} \right) y_{CO_2(n)} = 0 \quad (3.89)$$

At node the n^{th} node,

$$\left(\frac{D_{CO_2}}{\Delta Z^2} + \frac{u}{\Delta Z} \right) y_{CO_2(n-1)} + \left(-\frac{2D_{CO_2}}{\Delta Z^2} - \frac{u}{\Delta Z} - k_1 \right) y_{CO_2(n)} + \left(\frac{2u^2}{D_{CO_2}} \right) y_{CO_2(n+1)} = 0 \quad (3.90)$$

At the $(n + 1)^{th}$ node

$$\left(\frac{D_{CO_2}}{\Delta Z^2} + \frac{u}{\Delta Z} \right) y_{CO_2(n)} + \left(-\frac{2D_{CO_2}}{\Delta Z^2} - \frac{u}{\Delta Z} - k_1 \right) y_{CO_2(n+1)} + \left(\frac{2u^2}{D_{CO_2}} \right) y_{CO_2(n+2)} = 0 \quad (3.91)$$

For the last node $(n + 1)$, the discretized second boundary condition is applied (Pradeep, 2010);

$$\left(\frac{y_{CO_2(n+2)} - y_{CO_2(n)}}{2\Delta Z} \right) = 0 \quad (3.92)$$

This makes $y_{A(n+2)}$ equal to $y_{A(n)}$ and substituting for $y_{A(n+2)}$ at node $n + 1$

$$\left(\frac{2D_{CO_2}}{\Delta Z^2} + \frac{u}{\Delta x} \right) y_{CO_2(n)} + \left(-\frac{2D_{CO_2}}{\Delta x^2} - \frac{u}{\Delta x} - k_1 \right) y_{CO_2(n+1)} = 0 \quad (3.93)$$

At the first node, the following correlation is used to evaluate the coefficient;

$$y_{CO_2(1)} = \left(-\frac{2D_{CO_2}}{\Delta Z^2} - \frac{3u}{\Delta Z} - k_1 - \frac{2u^2}{D_{CO_2}} \right) \quad (3.94)$$

$$x_{CO_2(2)} = \left(\frac{2D_{CO_2}}{\Delta Z^2} + \frac{u}{\Delta Z} \right) \quad (3.95)$$

The coefficient of the right hand side of the equation is;

$$-\left(\frac{2u^2}{D_{CO_2}} + \frac{2u}{\Delta Z} \right) y_{CO_2(in)} \quad (3.96)$$

At the second node;

$$y_{CO_2(1)} = \left(\frac{D_{CO_2}}{\Delta Z^2} + \frac{u}{\Delta Z} \right) \quad (3.97)$$

$$y_{CO_2(2)} = \left(-\frac{2D_{CO_2}}{\Delta x^2} - \frac{u}{\Delta x} - k_1 \right) \quad (3.98)$$

$$y_{CO_2(3)} = \left(\frac{D_{CO_2}}{\Delta Z^2} \right) \quad (3.99)$$

The right hand side of the equation is equal to zero

At the 3rd node;

$$y_{CO_2(2)} = \left(\frac{D_{CO_2}}{\Delta Z^2} + \frac{u}{\Delta Z} \right) \quad (3.100)$$

$$y_{CO_2(3)} = \left(-\frac{2D_{CO_2}}{\Delta Z^2} - \frac{u}{\Delta Z} - k_1 \right) \quad (3.101)$$

$$y_{CO_2(4)} = \left(\frac{D_{CO_2}}{\Delta Z^2} \right) \quad (3.102)$$

The right hand side of the equation = 0

At node $n + 1$

$$y_{CO_2(n)} = \left(\frac{2D_{CO_2}}{\Delta Z^2} + \frac{u}{\Delta Z} \right) \quad (3.104)$$

$$y_{CO_2(n+1)} = \left(-\frac{2D_{CO_2}}{\Delta Z^2} - \frac{u}{\Delta Z} - k_1 \right) \quad (3.105)$$

The right hand of the equation = 0.

These coefficients are then arranged in tridiagonal matrix (A) and solved using a C++ code presented in appendix C.

**

CHAPTER FOUR-MATERIALS AND METHODS

4.1. Introduction

An experimental design is the most appropriate method used in the analysis of the optimization process. The Taguchi method was used to manipulate the experimental factors to generate statistically analyzable data where the choice of the factors being informed by the fact that the use of an experimental design dictates that the factors must have little or no degree of association. The effect of each factor in the response parameter $K_y a_e$, is established before optimization

4.2. Apparatus and materials

The absorption column

The design of this unit requires a sufficient understanding of the reaction kinetics, column hydrodynamics and mass transfer coefficients of the diffusing gas. These factors are important in simulation and optimization of the process (Haroun and Raynal, 2016). The column had an internal diameter of 0.15m, packed to a height of 0.35m. The height was so designed to achieve the objective of the process of producing biomethane of 95% methane at a negligible pressure drop across the bed. Glass spheres of diameter 0.04m was used as the column packing and provided a large surface area per unit volume in the bed where the fluids flowed in countercurrent.

The column had three distinct sections, the top section that had a liquid nozzle for an even distribution of the solvent stream over the bed's cross-section area, a middle section supported by a wire mesh and a bottom section having provision for gas inlet and distribution with a sump for draining the solvent.

Aqueous sodium hydroxide solution supply line

The solvent was held in the solvent tank and was pumped to the top of the column through a liquid rotameter by a 1/4' PVC pipes

Gas supply line

This line consisted of the biogas and carbon dioxide canisters that delivered the respective gasses, the gas rotameter and valves for flow regulation.

Gas analyzer

The gas analyzer was used to quantify CO₂ mole in the raw gas and the upgraded gas.

4.3. Experimental setup

The objective was realized by designing the absorption process such that the overall mass transfer coefficient $K_y a_e$, a parameter that is quantified using measurement of the CO₂ mole fraction in the gas to and from the column, is maximized. This was made possible by setting up an experiment as presented in the flow char in Figure 4.1. In this set-up, the effect of the four variable (experimental factors) on the following two parameters were investigated:

- 1) $K_y a_e$ which is the overall mass transfer coefficient based on the coefficient in the gas film,
- 2) a_e which is the effective mass transfer area for mass transfer over the packing surface.

The set-up was designed such that the gas and liquid flows in the packed bed are evenly distributed and regulated to avoid flooding or channeling (Hoffmann *et al.*, 2006). The experiments done by pumping the solvent to the top of the column at a fixed volumetric flow rate L , creating a solvent superficial velocity u_x in the bed while the raw gas was regulated by a valve, providing gas volumetric flow rate V , to the column.

The superficial velocities u_x and u_y were individually calculated assuming that the column was devoid of the packing and that the fluid was the only fluid flowing in the column. They were calculated using the following equations

$$u_x = (L/S) \text{ and } u_y = (V/S) \quad ()$$

Where S is base area of the column,

L is the solvent volumetric flow rate,

V is the gas volumetric flow rate.

To investigate the influence of the individual factors on the two parameters, one factor was varied over the set operating range while keeping the other factors constant. The operating range for each factor is given in Table 4.1.

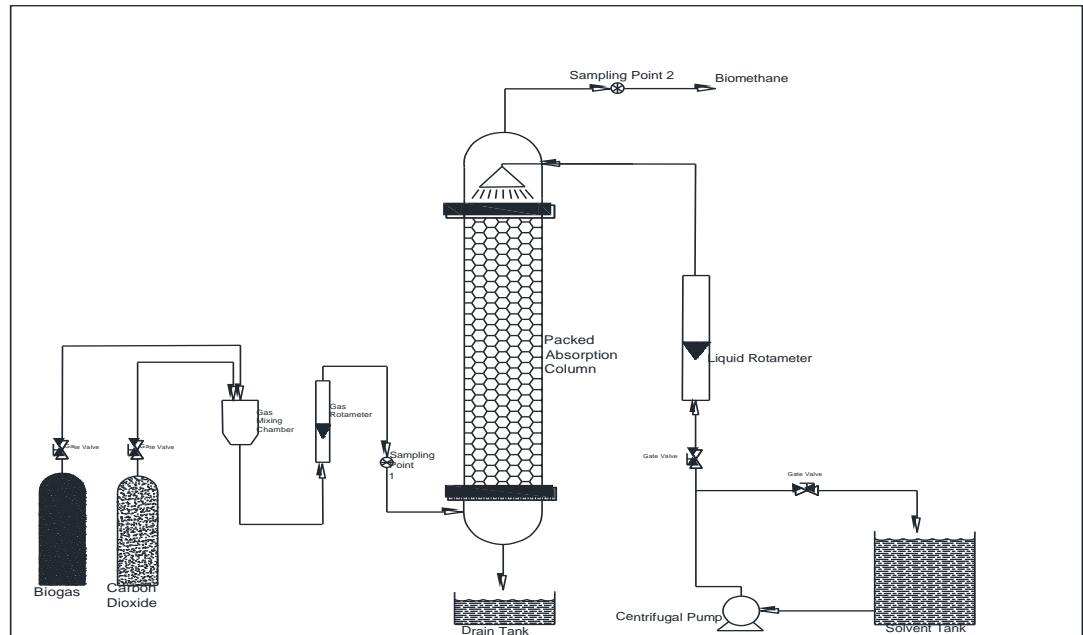


Figure 4. 1: Flow chart for biogas upgrading process

Table 4. 1: Region of interest for the experimental factors

Factors	Range	
	Low	High
Gas Superficial velocity, u_y (m/s)	0.5	2.5
Solvent Superficial velocity, u_x (m/s)	0.002	0.016
Solvent Concentration, OH^- (gmol/L)	0.1	0.3
CO_2 mole fraction in the gas feed (v/v)	0.45	0.55

4.4. Effective Area and Overall Mass Transfer coefficient

The two parameters are evaluated using Wang models from the previous chapter (section 3.3). for the effective mass transfer area over the packing (a_e) Eq. 3.53 is used while for the overall mass transfer coefficient ($K_y a_e$), Eq. 3.55a is used. The fractional effective area is the ratio of the effective area a_e , to the total surface area of the packing a_s , which was 5.06 m^2 .

$$a_f = (a_e/a_s) \quad (4.1)$$

4.5. Process Optimization

4.5.1. Parameter identification

There are many column variables that influence optimization of the chemisorption. However, this investigation considers the following variable as the experimental factors.

- i. Gas superficial velocity, u_y ,
- ii. Solvent superficial velocity, u_x ,
- iii. Solvent concentration, C_x ,
- iv. Carbon dioxide concentration in the gas feed, y_a .

These factors were subjected optimization using the Taguchi experimental design method within the ranges given in Table 4.1.

4.5.2. The experimental runs

Nine experiments were conducted based on a L_93^4 orthogonal array with the factors set at different levels for each run with the objective of maximizing $K_y a_e$ here considered to as the performance parameter. This parameter was calculated using CO_2 mole fraction in the gas to and from the column i.e. y_a and y_b respectively. These measurements were done using a gas analyzer respectively placed at sampling points 1 and 2 as identified in the flow sheet in Figure 4.1.

This was evaluated by the ascertaining the amount of CO_2 absorbed by the solvent using the ratio of CO_2 mole fraction in the gas stream to and from the column. The ratio was used in calculating the value of $K_y a_e$, using Eq. 3.55a and transformed to the signal-to-noise ratio ψ for statistical analysis.

4.5.3. The analysis of the response parameters

The objective here is to optimize the response parameter where, the objective function for optimization may be simplified as:

$$U(X_1, X_2, X_3, X_4) = \sum_{i=1}^4 U_i(X_i) \quad (4.2)$$

Where U is the optimum condition and X the experimental factors

The Taguchi method has created a standard orthogonal array to accommodate this optimization which is left to the researcher to select based on the number of factors, interactions and levels needed i.e. the number of different values the factor assumes according to its discretization within the *region of*

interest. Since there are four factors considered in the optimization with three levels, for each factor, the $L_9(3^4)$ orthogonal array was selected.

In this array, nine trials were sufficient to provide enough information for statistical analysis with each trial repeated five times and the average overall mass transfer coefficient $(K_y a_e)_n$ calculated. The coefficient was then transformed to the signal-to-noise ratio ψ_n for each trial. The concept of signal-to-noise ratio is useful in improvement of the quality through variability reduction and the improvement of measurement. From Table 3.1, the “*bigger-the-better*” objective function was used in calculating the averaged signal-to-noise ratios.

$$\psi = -10 \log \left[\frac{1}{n} \sum_{i=1}^n \left(\frac{1}{y_i^2} \right) \right] \quad (4.3)$$

Where y is the observed response parameter, the overall mass transfer coefficient

n is the number of repetitions in each trial,

Once the signal-to-noise ratio for the runs have been calculated, the averaged signal-to-noise ratio for each parameter at the three levels is estimated. This is done by averaging the signal-to-noise ratio where factor i at level j participated .

$$(\psi)_{i,j} = \left(\frac{(\psi)_1 + (\psi)_2 + (\psi)_3}{3} \right) \quad (4.4)$$

4.6. Calorific value measurement

The calorific values Q of the raw gas and the upgraded gas was established by conducting an experiment where a given mass of water is heated in a domestic stove fired by the gas for a period of time. In this experiments, 10 Kg of water was heated for 10 minutes and the rise in temperature $\Delta\theta$ noted. The gas to the stove was delivered as a volumetric flow rate of 0.05 m³/s of mass flow rate $V \cdot \rho$. The calorific value was then calculated by Eq. 4.1.

$$CV = (mc_p \Delta\theta) / (V \cdot \rho) \quad (4.5)$$

Where m is the mass water Kg,

c_p is the specific heat capacity of water $Kj \cdot Kg^{-1}K^{-1}$,

$\Delta\theta$ is the rise in temperature °C,

V is the flue gas volumetric flow rate , $m^3 \cdot s^{-1}$

ρ is the gas density $Kg \cdot m^{-3}$

**

CHAPTER FIVE-RESULTS AND DISCUSSIONS

5.1. A general view

Prior to establishing the optimum operating condition, the effect of the experimental factors on a_e , expressed as a fraction of the specific packing area (a_f), and the overall mass transfer coefficient ($K_y a_e$), are determined. Finally, the calorific values of the raw gas and the upgraded gas were then compared.

5.2. The fractional effective Mass Transfer area

5.2.1. Effect of solvent superficial velocity

The effect of the solvent superficial velocity (u_x), was investigated by increasing magnitude within the set range i.e. from 0.002 to 0.016 m/s . The calculated values of a_f , the effective area for mass transfer expressed as a fraction of the total surface area of the packing, was then plotted against u_x at different values of the gas superficial velocities u_y and the results presented in Figure 5.1.

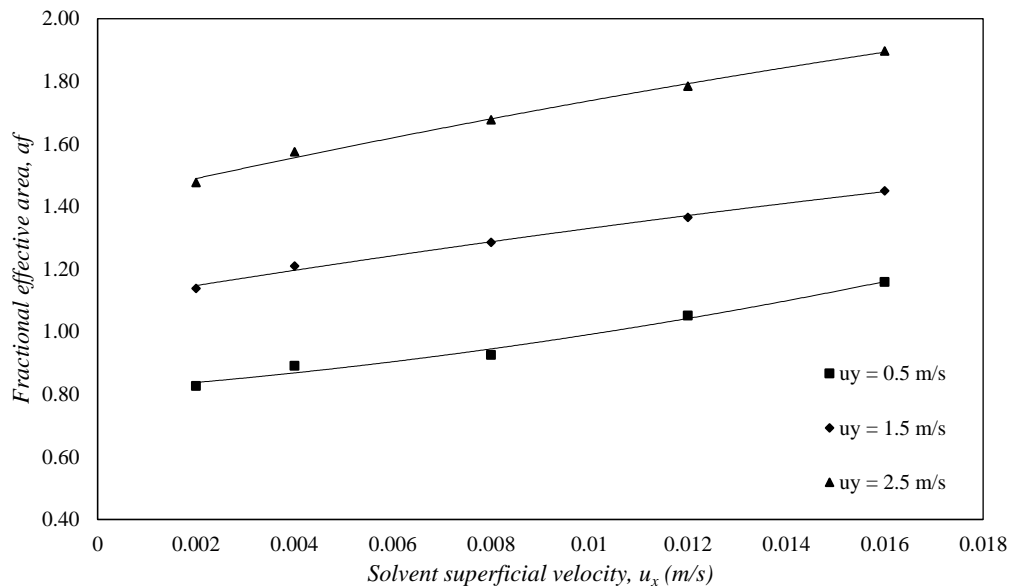


Figure 5. 1: Variation of the effective area with the solvent superficial velocity at three different gas superficial velocities.

From the plots, a_f , increased with increase in u_x . This increase is caused by an increase in the wetted area (a_w) over the packing and reduction in the magnitude of dead zones within the wetted surface. At high valued of u_x , turbulence is created in the liquid phase that creates disturbance at the

interface and formation of bubbles and mists, a phenomenon that increases the effective area for mass transfer a_e . As u_x increases, the rate of replacement of CO_3^{2-} ions in the reaction zone within the liquid film increases and going by the Le Chatelier's principle, this accelerates the forward reaction between CO_2 and $NaOH$.

Chao Wang (Wang, 2015), using MP250Y packing found that the effective area increased with increase in liquid superficial velocity to the power of 0.15 for all gas velocities.

5.2.2. Effect of Gas Superficial Velocity

With all the other factors kept constant, i.e. the solvent superficial velocity u_x , the solvent concentration $[OH^-]$ and CO_2 mole fraction y_a , the gas superficial velocity was increased from 0.5 to 2.5 m/s and the fractional effective area a_f , calculated over this range. Plots of a_f against u_y are generated for three different values of u_x as shown in Figure 5.2.

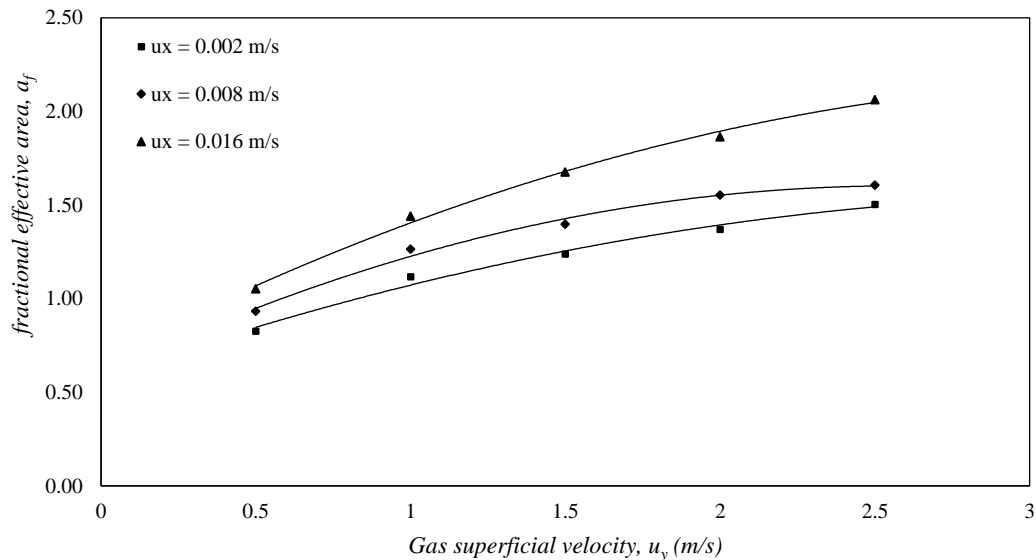


Figure 5. 2: The variation of fractional effective area (a_f) with the gas superficial velocity (u_y).

It is established that a_f increased with increase in u_y . This is attributed to the effect of increased instability of the liquid flow caused by the increased gas flow that lead to increased ripples, waves and droplets creation at the gas-liquid interface.

The increase in effective area with gas superficial velocity has also been observed by other researchers. It increases by 9% when the gas superficial velocity with increases from 0.59 to 1.48 m/s and increases by 2 to 3 % thereafter until flooding (Wang, 2015).

5.2.3. Effect of Solvent Concentration

The solvent concentration (OH^-), was increased from 0.1 to 0.3 $gmol/L$ while keeping all the other three factors constant, i.e. the gas superficial velocity u_y , the solvent concentration C_x and CO_2 mole fraction y_a . The fractional effective area a_f was then calculated over this range and plotted against the solvent concentration as presented in Figure 5.3. There is an increase in a_f with the solvent concentration caused by increased number of solvent molecules in the reaction zone. For a fast reaction, this zone is shifted towards the interface between the phases which increases the active sites at the this interface and subsequently increase a_e .

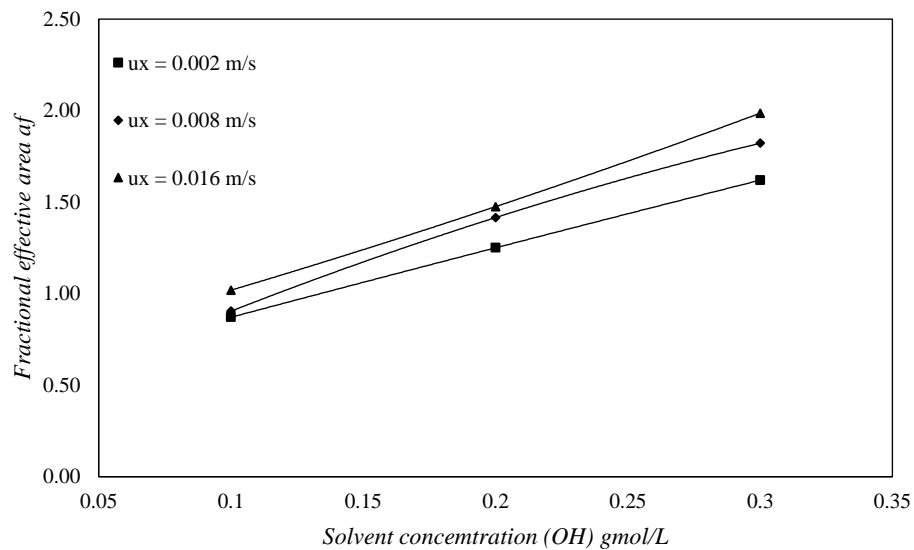


Figure 5. 3: A plot of the variation of fractional effective area with the solvent concentration at three different solvent superficial velocities.

5.2.4. Effect of carbon dioxide mole fraction

With solvent superficial velocity u_x , gas superficial velocity u_y , and the solvent concentration C_x kept constant, carbon dioxide mole fraction in the gas feed y_a , was increased 0.45 to 0.55 and the effective area a_f calculated and plotted against y_a as in the plots in Figure 5.4.

The fractional effective area increased with increase in y_a over the operating range. The increase is as a result of increased in solute concentration difference across the gas film that results in an increase in mass flux across the gas film. This creates the Marangoni effect, a condition of molecular instability at the interface which increases the magnitude of a_e .

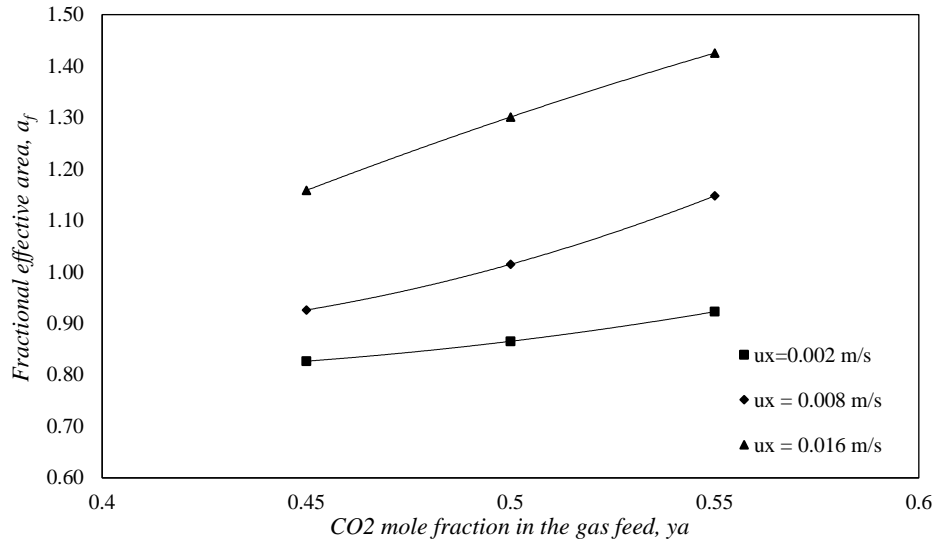


Figure 5. 4: Variation of the effective area with CO_2 mole fraction in the gas feed y_a

5.3. The Overall Mass Transfer Coefficient

5.3.1. Effect of solvent superficial velocity

The effect of the solvent superficial velocity (u_x) on $K_y a_e$ was evaluated by varying it over the operating range while keeping the other factors constant i.e. the gas superficial velocity u_y , solvent concentration C_x and CO_2 mole fraction y_a . The overall mass transfer coefficient $K_y a_e$, was then calculated and plotted against u_x in Figure 5.4.

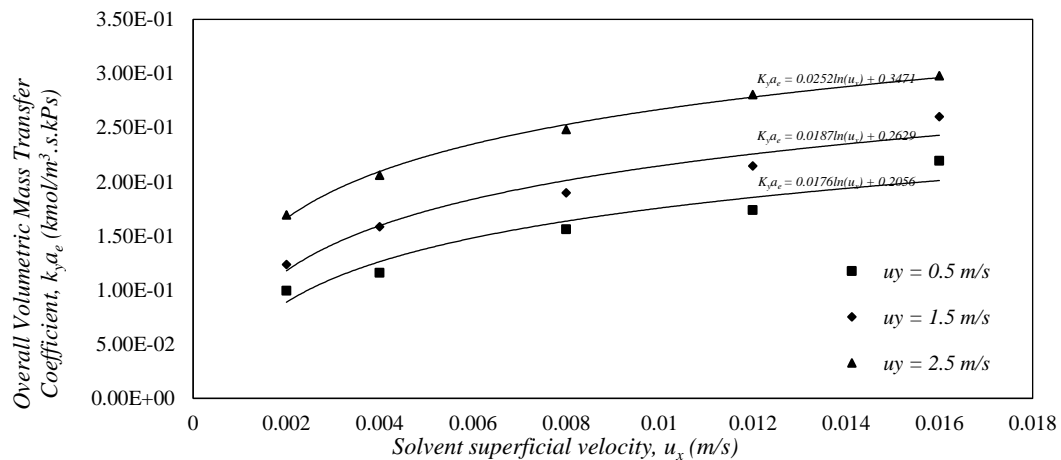


Figure 5. 5: Variation of the overall mass transfer coefficient with the solvent superficial velocity u_x .

The overall coefficient increased with increase in solvent superficial velocity at the three gas velocities caused by increased proportion of a_w , increased renewal of hydroxide molecules in the reaction zone and a reduction in liquid film resistance which increase $K_y a_e$.

5.3.2. Effect of gas superficial velocity

The gas superficial velocity u_y , was increased from 0.5 to 2.5 m/s, $K_y a_e$ was calculated over this range while keeping the solvent superficial velocity u_x , the solvent concentration $[OH^-]$ and CO_2 mole fraction y_a constant, and the results plotted in Figure 5.5. As u_y increases the overall coefficient increases, facilitated by turbulence in the gas phase which increases with u_y and the reduction of dead air zones unavailable for mass transfer, leading to an increase in gas film mass transfer coefficient k_y and subsequently $K_y a_e$. Depending on its magnitude, increase in u_y may also be responsible for increasing liquid phase turbulence.

The increase in interfacial area between the gas and liquid phases in the column has been reported to increase the magnitude $K_y a_e$. It increased from 23 to 34 kg-mol·(atm·m³·h)⁻¹ when the gas velocity increased from 2.3 to 6.2 m/s (Dixit, 2015). The same trend was observed by Sovilj *et al.*, (2019), who investigated the effect of gas superficial velocity at constant composition and solvent superficial velocity. The coefficient increased from 2.9 to 3.6 Kg, mol/(m²h) when the gas delivery was increased from 7,000 to 12,500 L/h similar trend had previously been observed by Charpentier, J. C., (1976).

5.3.3. Effect of Solvent Concentration

The solvent concentration (OH^-) was increased from 0.1 to 0.3 gmol/L while keeping the solvent superficial velocity u_x , gas superficial velocity u_y and CO_2 mole fraction y_a constant. The overall mass transfer coefficient $K_y a_e$ was calculated over this range and plotted against the concentration as presented in Figure 5.6. From the plots, $K_y a_e$ increases sharply with increase in $[OH^-]$, attributed to the influence of the reaction between the gas and the solvent whose rate is a function of the concentration of the reacting species. An increase in the solvent's concentration would increase the rate which in turn increases the enhancement factor β and contributes to an increase in the value of $K_y a_e$. The reaction zone within the liquid film is shifted towards the interface, having the effect of increasing the effective area a_e . This too contributes to increasing the overall coefficient.

Although an increase in concentration decreases the apparent gas phase mass transfer coefficient k'_y , due to an increase in solvent viscosity μ_x , the shift in the reaction zone towards the interface renders this effect insignificant.

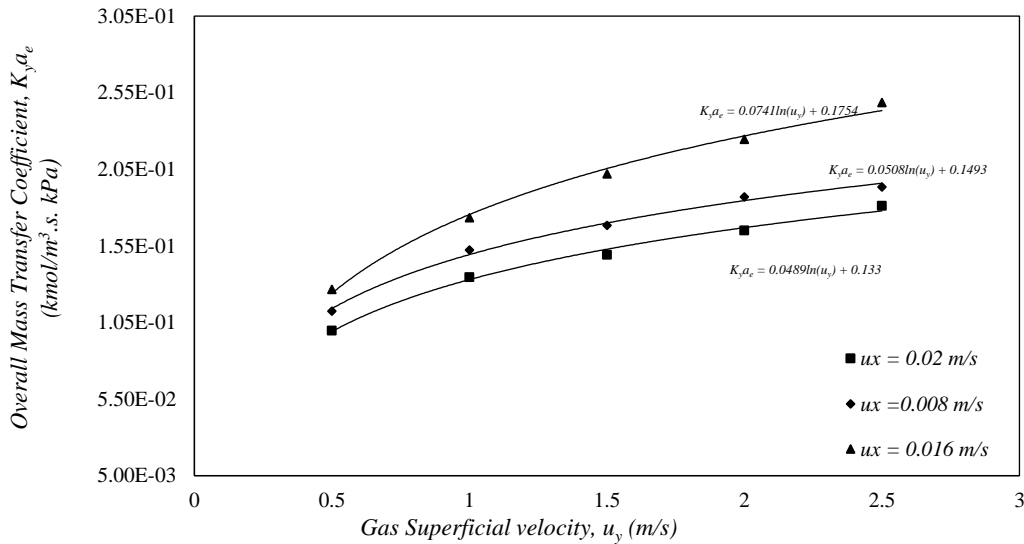


Figure 5. 6: Plot of the variation of the overall mass transfer with the gas superficial velocity u_y .

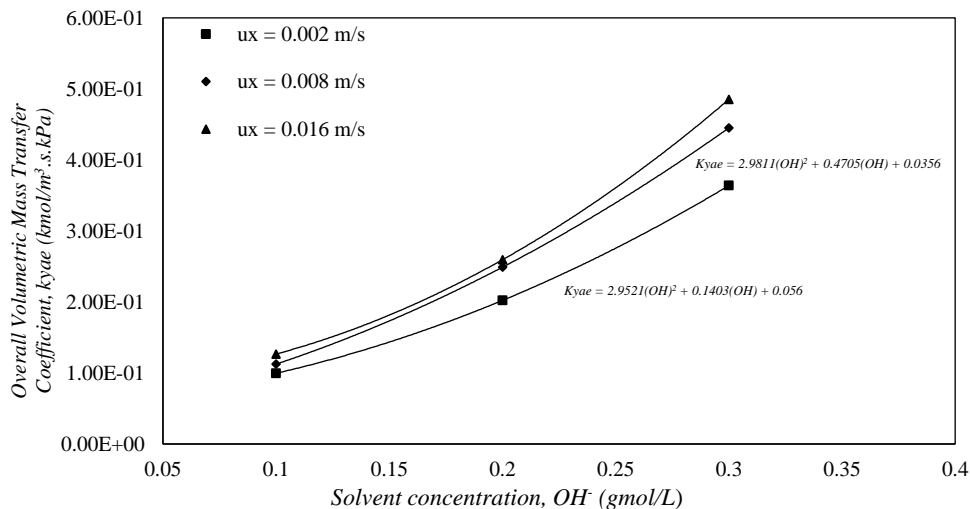


Figure 5. 7: Plot of the variation of $K_y a_e$ with the solvent concentration, $[OH^-]$

5.3.4. Effect of Carbon Dioxide Mole Fraction

The varying its value from 0.45 to 0.55, keeping the other three factors constant i.e. the solvent superficial velocity u_x , the gas superficial velocity u_y and the solvent concentration C_x . The calculated values of the $K_y a_e$ was plotted against y_a in Figure 5.7.

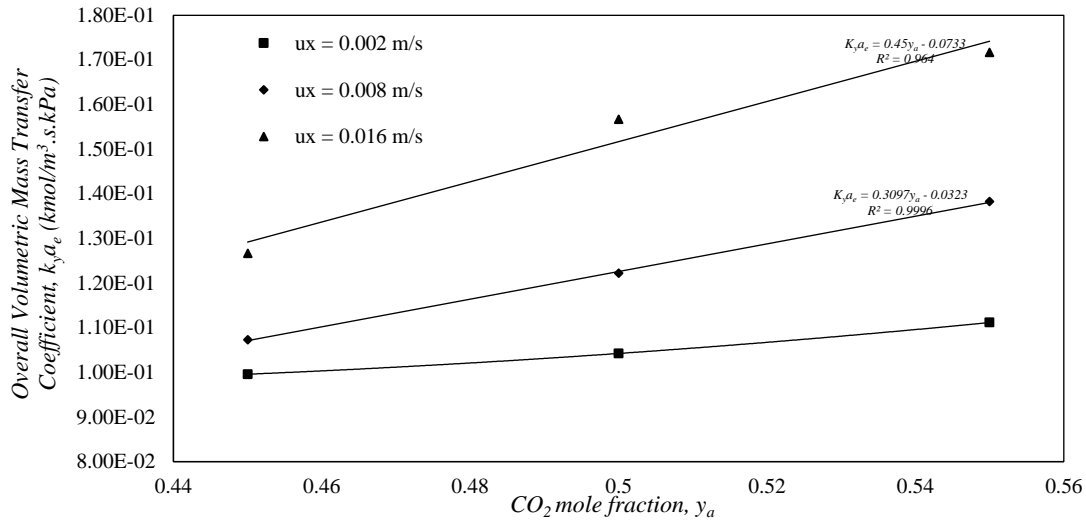


Figure 5. 8: Plot of the effect of CO_2 mole fraction on the overall mass transfer coefficient $K_y a_e$, at three different solvent velocities.

The overall coefficient increases marginally with increase in y_a . This is realized due to the increase in the gradient of CO_2 partial pressure in the gas film that increases molecular instability at the interface and the gas' concentration increase at the interface. The molecular instability stems from a variety of physio-chemical interaction that generates surface tension gradients, increasing molecular surface renewal. These scenarios increase the effective area a_e and subsequently $K_y a_e$. However, Sovilj *et al.*, (2019), found out that increasing CO_2 mole fraction in the gas feed at constant gas and solvent flow rates, the overall mass transfer coefficient decreases marginally.

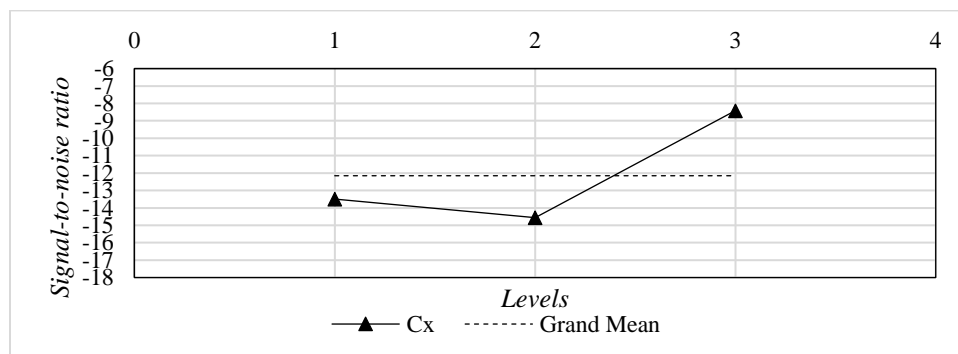
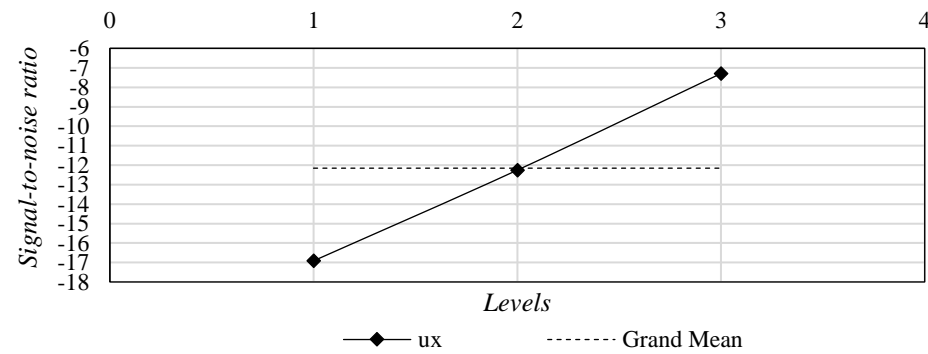
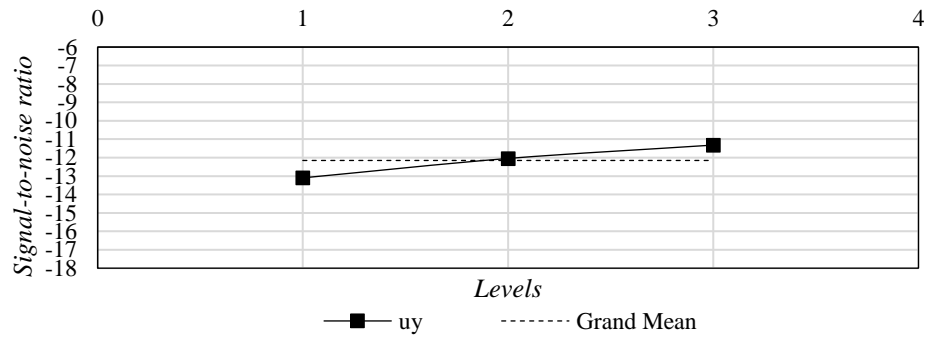
5.4. Process optimization

a) *The orthogonal array*

An $L_9(3^4)$ orthogonal array (OA) was used where nine experimental runs were performed with the factors set at three different levels. The response parameter was calculated for the nine experiments and tabulated in Table 5.1. The response parameters were converted to the signal-to-noise ratio ψ , for each run and the average value for each factor calculated based on the vales of ψ . Plots of ψ against the factor's levels were generated as presented in Figure 5.9.

Table 5. 1: The Response Parameters in an $l_9(3^4)$ Orthogonal Array.

Experiment Number	Independent Variables.				Averaged Performance Parameters	
	u_y	u_x	$[OH^-]$	y_a	y_b	$K_y a_e$ ($kmol/m^2 \cdot s \cdot kPa$)
1	1	1	1	1	0.0808	0.099017
2	1	2	2	2	0.0104	0.022335
3	1	3	3	3	0.0001	0.491151
4	2	1	2	3	0.2014	0.035657
5	2	2	3	1	0.1080	0.246973
6	2	3	1	2	0.0610	0.363912
7	3	1	3	2	0.2784	0.168839
8	3	2	1	3	0.2206	0.263379
9	3	3	2	1	0.0940	0.451447



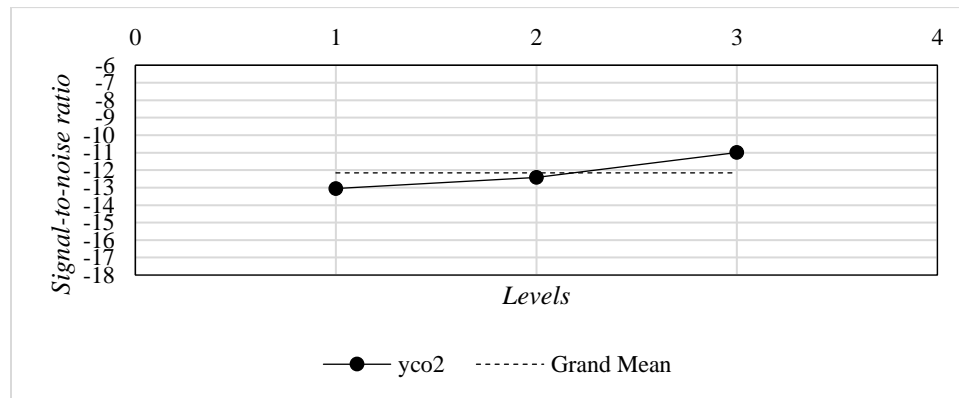


Figure 5. 9:Plots of the variation of the signal-to-noise ratios ψ , for the main effects for the experimental factors.

The influence of the factors is proportional to the magnitude of the plot and from the plots in Figure 5.9, solvent superficial velocity u_x , has the greatest influence while the gas superficial velocity u_y has the least. It is concluded that the column efficiency increases with increase in u_x . The optimum operating condition for the column is guided by the original objective function. Since the objective function was the “bigger-the-better” objective function. The optimum operating condition $\hat{\psi}$ is achieved when the factors are set at a level which gives the highest signal-to-noise ratio. In this case, the plots in the graph shows that all the factors are set at level 3 to attain optimum conditions. The levels are:

- i. u_y , at 2.5 m/s,
- ii. u_x at 0.016 m/s,
- iii. C_x at 0.3 gmol/L
- iv. y_a at 0.55 v/v

The optimum signal-to-noise ratio $\hat{\psi}$ was therefore -1.5539 , which transforms to the overall mass transfer coefficient of $0.8444 \text{ mol/m}^3 \cdot \text{s} \cdot \text{Pa}$.

b) The Analysis of variance (ANOVA)

As a follow up OA analysis, an analysis of variance ANOVA, is performed on the data where the importance of any of the factors is represented by the magnitude of the F – test value. The ANOVA results is presented in Table 5.4.

Table 5. 2: The ANOVA Table.

Factors	Degree of Freedom (DOF)	Sum of Squares (SS _f)	Mean Square	Variance ratio, (F)	Correction Factor (\bar{S}_f)	Percent contribution (ρ_f)
1 u_y	2	4.7940	2.3970	2.2309	2.6451	1.2235
2 u_x	2	139.0078	69.6039	64.6862	136.8588	63.3066
3 $[OH^-]$	2	64.6267	32.3134	30.0735	62.4778	28.9002
4 y_a	2	6.6810	3.3405	3.1089	4.5320	2.0963
Error	1	1.0745	1.0745			
Total	9	216.1840				

From the ANOVA table, the highest contribution to the signal-to-noise ratio ψ , is made by the solvent superficial velocity (u_x) whose contribution is 63.3% while the lowest is made by gas superficial velocity u_y at 1.22%. The significance of the factors measured by the F -test at a threshold of 4, show that y_a and u_y has no significant effect on the chemisorption of CO₂ in a packed column using aq NaOH solution.

c) *The optimum mass transfer coefficient*

Based on the analysis of ψ , the estimated value of the optimum operating conditions $\hat{\psi}$, was calculated. Based on the finding in Figure 5.9, the optimum operating condition is achieved when all the factors are set at level 3. i.e. u_y , at 2.5 m/s, u_x at 0.016 m/s, C_x at 0.3 gmol/L and y_{CO_2} at 0.55 v/v. The optimum signal-to-noise ratio $\hat{\psi}$, was evaluated to be -1.5539 , and it is transformed to a the overall mass transfer coefficient of value $0.8444 \text{ mol/m}^3 \cdot \text{s} \cdot \text{Pa}$.

5.5. The calorific value

The calorific values CV, of the raw gas and the upgraded gas were estimated using a domestic stove. For the raw biogas, the CV was 15,012.2 kJ/kg while that of upgraded biogas was 40,944 KJ/kg. This is an increase of 25,932.42 KJ/kg thanks to upgrading. However, the values recorded here are lower than the standard calorific values reported in literature and the discrepancy is attributed to heat losses in the stove.

5.6. Column simulation

The concentration profile of CO₂ in the bed with variation of gas superficial velocity u_y , was established by simulation of the CDR equation and presented in Figure 5.1.

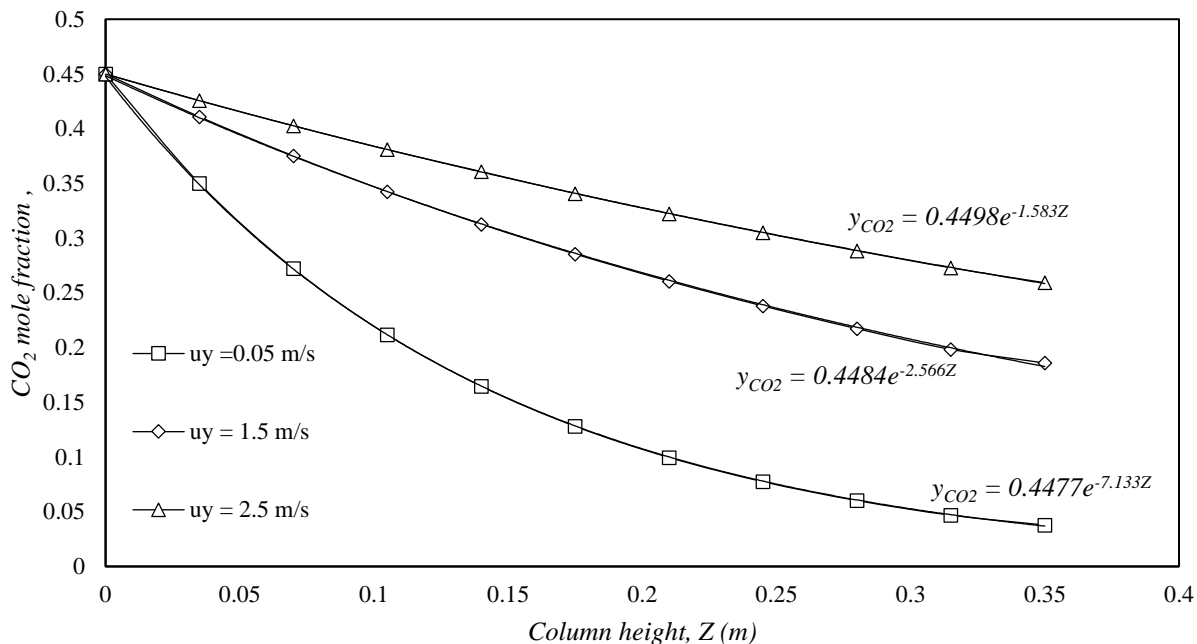


Figure 5.10: Simulated values of the variation of CO_2 along the column height Z with gas superficial velocity, u_y

The results show that there is a general exponential fall in CO_2 mole fraction. An increase in u_y increases the mole fraction in the exiting gas y_b . This finding informs the practice of keeping the gas flow rate to the column low, in the process increase the residence time in the column, in the process increase the amount of CO_2 being sequestered by the solvent. This will have the effect of increasing the column efficiency and reduce operating cost. The result of the model simulation of the model was compared with the experimental results and plotted in Figure 5.2.

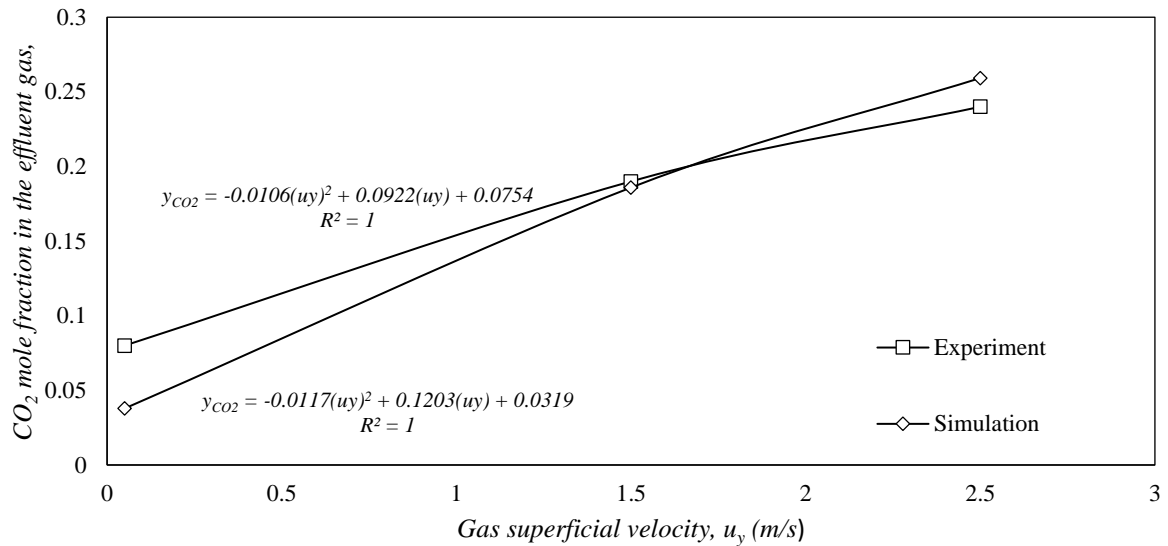


Figure 5. 11: Comparison of experimental and simulated values of y_b with gas superficial velocity.

Both results show that the effluent's CO_2 mole fraction increases with increase in u_y .

5.7. Hydrogen Sulphide sequestration

From all the experimental runs conducted the effluent gas from the column had no trace of H_2S according to the readings of the gas analyzer. It is then concluded that the dilute concentration of aq NaOH solution was effective in eliminating the poisonous gas from biogas.

**

CHAPTER SIX: - CONCLUSIONS AND RECOMMENDATIONS

6.1. Conclusions

Using the column's streams flow rates their concentrations, biogas was upgraded in a column packed with spherical packing operated at room temperature and pressure. Preceding the optimization, investigations were separately done to ascertain the effects of the experimental factors on the effective area for mass transfer a_e and the overall mass transfer coefficient $K_y a_e$. The following are the conclusions drawn:

I. Effective area,

- a) An increase in the solvent superficial velocity greatly influences the increase the effective area over the packing surface.
- b) An increase in the gas superficial velocity has a minimal effect on the effective area.
- c) Within the operating range of solvent concentration, the solvent concentration has no effect on the effective area.
- d) It was observed that variation of the concentration of carbon dioxide in the gas feed to the column has no effect in the effective areas for mass transfer.

II. Overall volumetric mass transfer coefficient

- a) The coefficient increases linearly with solvent superficial velocity of which the liquid film coefficient is a function of.
- b) As the gas velocity increases, the overall mass transfer coefficient increases linearly within the operating range.
- c) An increase in solvent concentration increases the overall mass transfer coefficient.
- d) The overall mass transfer coefficient decreases with increase in carbon dioxide mole fraction in the gas feed to the column.

III. Process optimization

Considering the four experimental factors, the solvent superficial velocity u_x had the highest influence on the overall mass transfer coefficient while the gas superficial velocity u_y had the least

effect. The ANOVA analysis further established that the gas superficial velocity u_y and CO₂ mole fraction in the gas feed y_a , have no significant effect of the operation of the column and for an optimum absorption, the liquid-to-gas L/G ratio must be kept high. A high ratio would eliminate the need of using a chemisorption process when upgrading the raw gas, making the process a purely a physical process while still retaining the benefits of eliminating the health hazard, increase calorific value and reduce CO₂ emission.

IV. Calorific value

Upgrading biogas using the reactive solvent increases its calorific value from an average of 15,012kJ/kg to an average value of 40,944 kJ/kg, justifying the upgrade.

6.2. Recommendation

6.2.1. Recommendations for work done

The recommendations drawn from the results of this investigative study is summarized as follows:

- i. Due to its low cost and simplicity, an absorption column should be incorporated to all existing and new biogas production plants.
- ii. To keep the operational cost low, a physical absorption could suffice. However, due to the presence of Hydrogen sulphide, the use of the solvent at low concentration is recommended.
- iii. The benefits of using the column are:
 - a) Reduce greenhouse gas emission
 - b) Increase calorific value for the fuel gas
 - c) Reduction in respiratory diseases
 - d) Reduced corrosion in machinery powered using biogas.

6.2.2. Recommendation for future work

- 1) Investigate column performance characteristics using CFD simulation software openFOAM.
 - i. access information on a local scale which is not measurable with experimental methods
 - ii. Use of turbulence models e.g. $k - \varepsilon$ model
- 2) This research has also elicited interest in simulating the randomly packed column using the Lattice Boltzmann method as is applied to porous media.

**

REFERENCES

- Abdeena, F. R. H, Mela, M., Jamia, M. S., Ihsanb, S. I., & Ismailb, A. F. (2017). Improvement of Biogas Upgrading Process Using Chemical Absorption at Ambient Conditions. *Jurnal Teknologi*. 1 November 2017. Retrieved from <https://www.researchgate.net/publication/321800687>
- Abd-Elhameed, W. N., Doha, E. H., & Youssri Y. H., (2013) New Wavelets Collocation Method for Solving Second-Order Multipoint Boundary Value Problems Using Chebyshev Polynomials of Third and Fourth Kinds. *Journal of Abstract and Applied Analysis* Volume 2013, Article ID 542839, 9 pages <http://dx.doi.org/10.1155/2013/542839>.
- Arora, S. & Kaur, I., (2015). Numerical solution of heat conduction problems using orthogonal collocation on finite elements. *Journal of the Nigerian Mathematical Society* 34 (2015) 286–302. Retrieved from www.sciencedirect.com on October 3, 2019.
- Ashgriz, A. N. & Mostaghimi J. (). Fluid Flow Handbook-An Introduction to Computational Fluid Dynamics. *Department of Mechanical & Industrial Eng. University of Toronto* Toronto, Ontario.
- Astarita, G., Savage, D. W., & Bisio, A., (1983) "Gas treating with chemical solvents" John Wiley.
- Athreya1, S. & Venkatesh, D. (2012). Application of Taguchi Method for Optimization of Process Parameters in Improving the Surface Roughness of Lathe Facing Operation. *International Refereed Journal of Engineering and Science (IRJES)* ISSN (Online) 2319-183X, (Print) 2319-1821 Volume 1, Issue 3 (November 2012), PP.13-19 www.irjes.com
- ATSDR-Agency for toxic substance and disease registry (2010). Medical Management Guidelines for Hydrogen Sulfide. Retrieved February 3-2018 from <https://www.atsdr.cdc.gov/mmg/mmg.asp?id=385&tid=67>.
- Haddadi, B., Jordana, C., Hamid, R., Harasek, N. M., (2016). Investigation of the Pressure Drop of Random Packed Bed Absorbers. *Chemical engineering transactions* vol. 52, 2016. ISBN 978-88-95608-42-6; ISSN 2283-9216
- Bani-Ahmad, A. K., Alomari1, A., Sami, B. J., & Hashim, S. I., (2016). On the approximate solutions of systems of odes by Legendre operational matrix of differentiation. *Italian journal of pure and applied mathematics* – n. 36–2016 (483–494)
- Beygi, N. S., Hakimzadeh, H. & Chenaglou, M. R., (2014). Simulation of free surface flows using volume of fluid method and genetic algorithm. *Journal of Hydroinformatics*, September 2014. doi: 10.2166/hydro.2014.152
- Bhusare, V. H., Dhiman, M. K., Kalaga, D.V., Roy, S. & Joshi, J. B. (2017). CFD simulations of a bubble column with and without internals by using OpenFOAM *Chemical Engineering Journal* 317 (2017) 157–174

- Billet, R. & Schiltes, M., (1999). Prediction of mass transfer columns with dumped and arranged packings. *Institution of chemical engineers*. Trans I Chem E, Vol 77, Part A, September 1999.
- Blau, G., Lasinski, M., Orcun, S., HuanHsu, S. Caruthers, J., Delgass, N. & Venkat Venkatasubramanian (2008). High fidelity mathematical model building with experimental data: A Bayesian approach. *Computers & Chemical Engineering* Volume 32, Issues 4–5, 5 April 2008, Pages 971-989. Retrieved on March 16, 2018 from: <https://www.sciencedirect.com/science/article/pii/S0098135407000968>
- Boiarkine, O., Kuzmin, D., Canic, S., Guidoboni, G. & Mikelic, A. (2011). A positivity-preserving ALE finite element scheme for convection–diffusion equations in moving domains. *Journal of Computational Physics* 230 (2011) 2896–2914.
- Cavazzuti, M., (2015). Optimization Methods: From Theory to Design, 13 DOI: 10.1007/978-3-642-31187-1_2, Springer-Verlag Berlin Heidelberg 2013 <https://www.researchgate.net/publication/261750290>.
- Chen, P. C. & Lin, S. Z. (2018). Optimization in the Absorption and Desorption of CO₂ Using Sodium Glycinate Solution. *Appl. Sci.* 2018, 8, 2041; doi:10.3390/app8112041.
- Chidambaram, M., (2018). Mathematical Modelling and Simulation in Chemical Engineering. First Edition, Cambridge University Press, pp 135.
- Coulson, L., M. & Richardson, J. F. (1999). Chemical Engineering – Fluid Flow, Heat Flow and mass Transfer. Volume 1, 6th Edition. Chapter 10. *Butterworth Heinemann* ISBN 0-7506-4444-3.
- Coulson, L.M. & Richardson, J. F. (1992). Chemical Engineering- Particle Technology. Volume 2, 4th Edition. *Butterworth Heinemann* ISBN 0-7506-2942-8.
- Dagde, K. K. & Akpa, J. G., (2014). Numerical Simulation of an Industrial Absorber for Dehydration of Natural Gas Using Triethylene Glycol. *Journal of Engineering* Volume 2014, Article ID 693902, 8 pages <http://dx.doi.org/10.1155/2014/693902>
- Danckwerts, P.V., (1970). Gas Liquid Reactions. *McGraw-Hill*, pp. 276-302.
- Ludington, D. (2013). Calculating the Heating Value of Biogas. Retrieved on March 16, 2018 from: masters.donntu.org/2013/fkita/alexandrova/.../Heating_Value_of_Biogas_copy.pdf
- Davis, R. & John, P., (2018). Application of Taguchi-Based Design of Experiments for Industrial Chemical Processes. *Statistical Approaches with Emphasis on Design of Experiments Applied to Chemical Processes. (Chapter 9)*. Downloaded from: <http://www.intechopen.com/books/statistical-approaches-with-emphasis-on-design-of-experiments-applied-to-chemical-processes>.
- Piro, D. J. & Maki, K. J. (2013). An adaptive interface compression method for water entry and exit. *University of Michigan Department of Naval Architecture and Marine Engineering*, No. 2013-350.
- Durakovic, B. (2017). Design of Experiments Application, Concepts, Examples: State of the Art. *Periodicals of Engineering and Natural Sciences* ISSN 2303-4521 Vol 5, No 3, December 2017, pp. 421–439. Retrieved on June 1, 2021, from: <http://pen.ius.edu.ba>.
- Dwivedi, A., & Das, D., (2015). Application of Taguchi Philosophy for Optimization of Design Parameters in a Rectangular Enclosure with Triangular Fin Array. *J. Inst. Eng. India Ser. C* (October–December 2015) 96(4):351–362 DOI 10.1007/s40032-015-0186-9
- Environmental defense fund (2017) Methane: The other important greenhouse gas. Retrieved on December 30-2017 from <https://www.edf.org/methane-other-important-greenhouse-gas>.
- Eyer, F & Zilker, T. (2009), Caustic injuries of the eye, skin and the gastrointestinal tract. *The Umsch* 2009 May; 66(5):379-86. doi: 10:1024/0040-5930.66.5.3790

- Fei, N. C., Mehat, N. M. & Kamaruddin, S. (2013). Practical Applications of Taguchi Method for Optimization of Processing Parameters for Plastic Injection Moulding: A Retrospective Review. *ISRN Industrial Engineering* Volume 2013, Article ID 462174, 11 pages <http://dx.doi.org/10.1155/2013/462174>
- Flagiello, D., Parisi, A., Lancia, A., & Natale, D. F., (2021). A Review on Gas-Liquid Mass Transfer Coefficients in Packed-Bed Columns. *ChemEngineering* 2021, 5, 43. <https://doi.org/10.3390/chemengineering5030043>
- de Vuyst, F., (2013). Numerical modeling of transport problems using freefem++ software – with examples in biology, CFD, traffic flow and energy transfer. Master. Modélisation numérique des problèmes de transport sur freefem++, *ENS CACHAN*, 2013, pp.162. cel-00842234.
- Garcia, G. E. C., van Eeten, K. M.P., de Beer, M. M., Schouten, J. C., & van der Schaaf, J., (2018). On the Bias in the Danckwerts' Plot Method for the Determination of the Gas-Liquid Mass-Transfer Coefficient and Interfacial Area. *MDPI*, Accessed January 26, 2021.
- Gheni, S. A, Abed. M. F, Halabia. E. K, & Ahmed. S. R (2018). Investigation of carbon dioxide (CO₂) capture in a falling film contactor by computer simulation. *Oil & Gas Science and Technology - Revue d'IFP Energies nouvelles*, Institut Français du Pétrole, 2018, 73, pp.43. 10.2516/ogst/2018020. hal-0190284.1
- Global Legal Insight, 2018. Energy Kenya-An overview of the current energy mix, and the place in the market of different energy sources. Retrieved on February 23, 2018 from <https://www.globallegalinsights.com/practice-areas/energy-laws-and.../kenya>
- Grazia, L., (2014). Upgrading of biogas to bio-methane with chemical absorption process: simulation and environmental impact. *Journal of Cleaner Production*. Retrieved on October 25, 2017 from <https://doi.org/10.1016/j.jclepro.2016.05.020r>.
- Greenbrick eco-solutions (2018). Renewable Natural Gas - Bio CNG. Retrieved on February 3, 2018 from www.gbcs.in.
- Hanley, B., Dunbobbin, B. & Bennett, D., (1994). A Unified Model for Countercurrent Vapor/Liquid Columns. 1. Pressure Drop. *Ind. Eng. Chem Res.* 1994, 33, 1208-1221. Doi:10.1021/ie00029a017
- Hansen, C. M. (2007). Hansen Solubility Parameters. A user's hand book, Second ed., CRC Press, *Taylor & Francis Group*, 2007.
- Haroun, Y., Ludovic, R. & Cécile, P., (2013). Pressure drop and effective area predictions in structured packings using CFD. *Récents Progrès en Génie des Procédés, Numéro 104 - 2013* ISSN: 1775-335X ; ISBN: 978-2-910239-78-7, Ed. SFGP, Paris, France.
- Haubrock, J., Hogendoorn, J. A., & Versteeg, G. F. (2005). The Applicability of Activities in Kinetic Expressions: a More Fundamental Approach To Represent the Kinetics Of the System CO₂-OH- In Terms Of Activities. *International Journal of Chemical Reactor Engineering*. DOI 10.2202/1542-6580.1290.
- Hegely, L., Roesler, J., Alix, P., Rouzineau, D., & Meyer. M., (2017). Absorption methods for the determination of mass transfer parameters of packing internals: A literature review. *AIChE Journal*, Wiley, 2017, 63 (8), pp.3246-3275. 10.1002/aic.15737. hal-01587673
- Kimweri, H. T. H., (2001). Enhancement of gas-liquid mass transfer in hydrometallurgical leaching systems.(Doctoral dissertation, *University Of British Columbia*, 2001) Retrieved on August 14-2018 from www.sciencedirect.com
- Hirt, C., Hirt, W. & Nichols, B.D. (1981). Volume of Fluid (VOF) Method for the Dynamics of Free Boundaries. *Journal of computational physics* 39, 201-225 (1981)
- Hivos (2018). Kenya: Energy Profile. Retrieved on January 26, 2018 from https://www.hivos.org/sites/default/files/kenya_profile.pdf

- Hoffmann, A. B., Hupen, A., Loning J. M., Haas, M., Bukowski, T., & Hallenberger, K. (2016). Standardization of mass transfer measurements—a basis for the description of absorption processes. *Institution of Chemical Engineers*. Symposium Series no. 152 # 2006. Retrieved on February 18 2018 from: folk.ntnu.no/skoge/prost/proceedings/distillation06/CD-proceedings/paper049. pd.
- Hou, S., S., Chiang, C. Y., & Lin, T., H., (2020). Oxy-Fuel Combustion Characteristics of Pulverized Coal under O₂/Recirculated Flue Gas Atmospheres. *Applied sciences*. 2020, 10, 1362
- Huertas, J. I., Giraldo, N & Izquierdo, S., (2014) Removal of H₂S and CO₂ from Biogas by Amine Absorption. *Automotive Engineering Research Center-CIMA of Tecnologico de Monterrey, Mexico*. Retrieved on February 5, 2018 from <http://www.intechopen.com/books/mass-transfer-in-chemical-engineeringprocesses/removal-of-h2s-and-co2-from-biogas-by-amine-absorption>.
- Hupen, B., Hoffmann, A., Gorak, A., Loning, J. M., Haas, H., Runowski, T., Hallenberger, K., (2018). Standardization of mass transfer measurements – a basis for the description of absorption processes. *IChemE*, 2006. SYMPOSIUM SERIES NO. 152. Retrieved on march 15, 2018 from: folk.ntnu.no/skoge/prost/proceedings/distillation06/CD-proceedings/paper049. pd.
- International energy agency (2014) African energy outlook Retrieved on February 23, 2018 from <https://www.iea.org/weo2014>.
- International energy agency (2017) World energy outlook Retrieved on February 23, 2018 from <https://www.iea.org/weo2017>.
- International Labmate Limited Biogas (2010) Desulphurization System Reduces Costs at Waste Management Site. Retrieved on February 5, 2018 from https://www.envirotech-online.com/news/air-monitoring/6/.../biogas..._/28838
- Fair, J. A., & Steinmeyer, D. E., Penney, W. R., & Crocker, B. B., (1997). *Perry's Chemical Engineer's Handbook* 7th Edition New York: McGraw-Hill.
- Jansen, D., Gazzani, M., Manzolini, G., van Dijk, E., & Carbo, M., (2015). Pre-combustion CO₂ capture. *International Journal of Greenhouse Gas Control*. 40 (2015) 167-187
- Cooke, J. (2016). Modelling of reactive absorption in gas-liquid on structured packing. PhD Dissertation. *University of Southampton Repository*, 2016
- Bao, D & Singh, R., (2018). Device-scale CFD study for mass transfer coefficient and effective mass transfer area in packed column. Pacific Northwest National Laboratory Richland, Washington 99352 PNNL – 28161
- Miller, J. D. & Rehm, T. R., (1998). Packed column mass transfer coefficients for concurrent and countercurrent flow: An analysis of the recent work. *University of Arizona*. Retrieved on October 21, 2017 from calliope.dem.uniud.it/CLASS/IMP-CHIM/C8-Cussler.pdf
- Jørgensen, P. J., (2009). PlanEnergi and Researcher for a Day Faculty of Agricultural Sciences, *Aarhus University* 2009 2nd edition. ISBN 978-87-992243-2-1 Retrieved on December 22,2017 from www.dca.au.dk/fileadmin/DJF/Kontakt/Besog.../Biogas-Green Energy 2009 AU.pdf.
- Kamaruddin, S., Khan, Z. A. & Wan, K. S. (2004). The use of the Taguchi method in determining the optimum plastic injection molding parameters for the production of a consumer product. *Jurnal Mekanikal* Desember 2004, Bil.18, 98 – 110.
- Hemminki, K. & Marja-Liisa, N. (1982). Community study of spontaneous abortions: Relation to occupation and air pollution by sulfur dioxide, hydrogen sulfide, and carbon disulfide. *International Archives of Occupational and Environmental Health*. Volume 51, Issue 1, pp 55–63. Retrieved on February 10, 2018 from: <https://link.springer.com/article/10.1007/BF00378410>

- Karunaratne, S., Eimer, D. & Erik, L. O., (2014), Model Uncertainty of Interfacial Area and Mass Transfer Coefficients in Absorption Column Packing. *Proceedings of the 58th SIMS*, September 25th - 27th, Reykjavik, Iceland.
- Kelishami, A. R., Bahmanyar, H. & Hajamini, Z., (2015). A novel approach for calculating packed column height based on new correlation of mass transfer coefficient. *Polish Journal of Chemical Technology*, 17, 1, 48 — 54, 10.1515/pjct-2015-0008.
- Kenig, E. & Seferlis, P. (2009). Modelling reactive absorption. January 2009 retrieved from www.aiche.org/cep
- Kierzkowska-Pawlak, H., (2012). Determination of kinetics in gas-liquid reaction systems. An overview. *Ecol Chem Eng s.* 2012; 19(2):175-196. DOI: 10.2478/v10216-011-0014-y
- Kim, A. S., (2020). Complete analytical solution for convection-diffusion-reaction-source equations without using an inverse Laplace transform. *Scientific reports.* (2020) 10:8040 | <https://doi.org/10.1038/s41598-020-63982-w>
- Kimweri, H. T. H., (2001). Enhancement of gas-liquid mass transfer in hydrometallurgical leaching systems. PhD dissertation, 2001. *University of British Columbia*.
- Knuutila, H., Juliussen, O., & Svendsen, H. F. (2010). Kinetics of the reaction of carbon dioxide with aqueous sodium and potassium carbonate solutions. *Chemical Engineering Science* 65(23), 6077-6088.
- Kooijman, H. A., (1995). Dynamic Non-Equilibrium Column Simulation. PhD Dissertation, Clarkson University 1995
- Kukreja, A., Chopra, P., Aggarwal, A. & Khanna, P., (2011). Application of Full Factorial Design for Optimization of Feed Rate of Stationary Hook Hopper. *International Journal of Modeling and Optimization*, Vol. 1, No. 3, August 2011
- Kumar, R. K., Rao, R. V. R., Sankarshana, T. & Khan, A., (2012). Liquid Holdup in Concurrent Gas Liquid Upflow Through Packed Column with Random and Corrugated Structured Packing. *Proceedings of the World Congress on Engineering and Computer Science 2012 Vol II*. WCECS 2012, October 24-26, 2012, San Francisco, USA.
- Lewis, W., & Whitman, W. (1924). Principles of gas absorption, *Industrial & Engineering Chemistry* 16(12), 1215-1220.
- Yang, L., Liu, F., Saito, K. & Liu, K., (2018) Modeling on Hydrodynamic Characteristics of Multiphase Counter-Current Flow in a Structured Packed Bed for Post-Combustion CO₂ Capture. *Journal Energies* 2018
- Linek, V., Moucha, T. & Rejl, F. J., (2001). Hydraulic and mass transfer characteristics of packings for absorption and distillation columns. Rauschert-Metall-Sattel-Rings. *Trans IChemE.* 2001;79: 725-732.
- Lynn, S, Straatemeier, J. R. & Kramers, H. (1955). Absorption studies in the light of the penetration theory: I. Long wetted-wall columns. *Chemical Engineering Science* Volume 4, Issue 2, April 1955, Pages 49-57.
- Maheswari, C., Krishnamurthy, K. & Parameshwaran, R., (2014). Modeling and experimental analysis of packed column for SO₂ emission control process. *Atmospheric Pollution Research* 5(2014) 464 470.
- Maryam, M & Keith, D. W., (2009). Low-energy sodium hydroxide recovery for CO₂ capture from atmospheric air—Thermodynamic analysis. *International Journal of Greenhouse Gas Control*
- Maile, O. I., Tesfagiorgis, H. B., & Muzenda, E., (2015). Factors Influencing Chemical Absorption of CO₂ and H₂S in Biogas Purification: A Review. *Proceedings of the World Congress on Engineering and Computer Science 2015 Vol II WCECS 2015*, October 21-23, 2015, San Francisco, USA.
- Maile, Q., Tesfagiorgis, H. B & Muzenda, E., (2015). Factors Influencing Chemical Absorption of CO₂ and H₂S in Biogas Purification: A Review. *Proceedings of the World Congress on Engineering and Computer*

- Science* 2015. Vol II. WCECS 2015, October 21-23, 2015, San Francisco, USA. Retrieved on February 10, 2018 from www.iaeng.org/publication/WCECS2015/WCECS2015_pp619-622.pdf
- Makaruk, A., Miltner, M. & Harasek, M., (2010). Membrane biogas upgrading processes for the production of natural gas substitute. *Separation and Purification Technology* 74 (2010) 83–92. Retrieved on March 25, 2018 from www.elsevier.com/locate/seppur.
- Mangers, R. J. & Ponter, A. B., (1980). Effect of viscosity on liquid film resistance to mass transfer in a packed column. *Ind. Eng. Chem. Process Des. Dev.* 1980; 19: 530-537.
- Kajotonia, M. M., (2008). . Comparative Study of Collocation Methods for the Numerical Solution of Differential Equations. PhD Dissertation. School of Mathematical Sciences, *University of KwaZulu Natal* 2008.
- Mendes, M. F., (2011). HETP Evaluation of Structured and Randomic Packing Distillation Column. Chemical Engineering Department, Technology Institute, *Universidade Federal Rural do Rio de Janeiro Brazil*. Retrieved on March 15, 2018 from cdn.intechopen.com/pdfs/22865.pdf
- Mehrara, H., Roozbehani, B., Shishehsaz, M. R., Mirdrikvand, M. & Moqadam S. I., (2012). Using Taguchi method to determine optimum process conditions for flue gas desulfurization through an amine scrubber. *Clean Techn Environ Policy* DOI 10.1007/s10098-013-0593-7
- Mehrara, H., Roozbehani, B., Shishehsaz, R., Mirdrikvand, M. & Moqadam, S. I, (2013). Using Taguchi method to determine optimum process conditions for flue gas desulfurization through an amine scrubber. *Clean Techn Environ Policy* DOI 10.1007/s10098-013-0593-7
- Mehryar, E., Ding W., Hemmat A., Hassan M., Talha Z., Kafashan J., & Huang H., (2017). Modeling and Multiresponse Optimization for Anaerobic Codigestion of Oil Refinery Wastewater and Chicken Manure by Using Artificial Neural Network and the Taguchi Method. *Hindawi BioMed Research International* Volume 2017, Article ID 2036737, 15 pages <https://doi.org/10.1155/2017/2036737>.
- Harasek, M. & Makaruk, A., (2013). New developments in Biogas upgrading (in Austria), task37. Retrieved on December 30, 2017 from www.ieabioenergy.com/files/daten-redaktion/.../2/Makaruk_Harasek_vienna.pdf.
- Hughes, M. J., 2010. Optimisation of Complex Distillation Column Systems using Rigorous Models. PhD Dissertation, *University of Cape Town* 2010
- Parti, M., (1994). Mass Transfer Blot Numbers. *Periodica Polytechnica Ser. Mech. Eng.* VOL. 38, NOS. 2-9, PP. 109-122 (1994)
- Mir, M. A., Hussain, A. & Verma. C., (2016). Design considerations and operational performance of anaerobic digester: A review. *Cogent Engineering* (2016), 3: 1181696. Retrieved on February 5, 2018 from <http://dx.doi.org/10.1080/23311916.2016.1181696>.
- Mirzaei, S., Shamiri, A., & Aroua, M. K., (2015). A review of different solvents, mass transfer, and hydrodynamics for post combustion CO₂ capture. Retrieved on August 22, 2018 from <http://umexpert.um.edu.my>
- Molstad, M. C., McKinney, J. F. & Abbey, R. G., (1943). Performance of drip-point grid tower packing, III Gas-film mass transfer coefficients: additional liquid film mass transfer coefficients. *Trans. Am Inst. Chem. Eng* 39(1943) 605.
- Muhammad, N., Manurung, Y., Hafidzi, M., Abas, S. K., Tham, G. & Rahim, M. R. A., (2012). A Quality Improvement Approach for Resistance Spot Welding using Multi-objective Taguchi Method and Response Surface Methodology. *International Journal on Advance Science Engineering Information Technology*. Vol. 2(2012) No 3 ISSN: 2088-5334.
- Mustafa, N. F. A., Shariff, A. M. S., Tay, W. H., Halim, H. N. A. & Yusof, S. M. M. (2010). Mass Transfer Performance Study for CO₂ Absorption into Non-Precipitated Potassium Carbonate Promoted with

- Glycine Using Packed Absorption Column. *Multidisciplinary Digital Publishing Institute (MDPI)*, 9 May 2020.
- Nair, P. S. & Selvi. P. P., (2014). Absorption of Carbon dioxide in Packed Column. *International. Journal of Scientific and Research Publications*, Volume 4, Issue 4, April 2014 1 ISSN 2250-3153. Retrieved on December 23, 2017 from www.ijsrp.org/research-paper-0414/ijsrp-p2885.pdf.
- Najib, S. B. M., Kamarudin, K. S. N & Dolmat, N., (2015). Methyl-diethanolamine and Piperazine as Extractant in Emulsion Liquid Membrane for Carbon Dioxide Removal. *International Journal of Chemical Engineering and Applications*, Vol. 6, No. 5, October 2015. Retrieved on January 17, 2018 from www.ijcea.org/vol6/502-N0008.pdf
- Nalbant, M., Gokkaya, H., & Sur, G., (2007). Application of Taguchi method in the optimization of cutting parameters for surface roughness in turning. *Materials and Design* 28 (2007) 1379–1385
- Nathalie, J. M. C., Penders-van, E., Hamborg, E. S., Huttenhuis, P. J. G., Fradette, S, Carley, J. A & Versteeg, G. F., (2012). Eleventh Annual Carbon Capture, Utilization & Sequestration Conference – April 30-May 3, 2012
- National Environment Management Authority (NEMA). The national solid waste management strategy-201. From: www.nema.go.ke. Retrieved on February 22, 2018.
- National Oceanic and Atmospheric Administration (NOAA).(March 12, 2018). Mauna Loa. *Hawaii Observatory Report*. Retrieved on March 12, 2018 from <https://www.esrl.noaa.gov/gmd/obop/mlo>
- Ghasem, N., (2019). Modeling and Simulation of the Absorption of CO₂ and NO₂ from a Gas Mixture in a Membrane Contactor. *MDPI-Processes* 2019, 7, 441; doi:10.3390/pr7070441
- Ndiritu, H. M., Kibicho. K., & Gathitu, B. B., (2013) Influence of Flow Parameters on Capture of Carbon Dioxide Gas by a Wet Scrubber. *Journal of Power Technologies* 93 (1) (2013) 9–15. Retrieved on January 05, 2018 from: <http://papers.itc.pw.edu.pl/index.php/JPT/article/download/332/513>
- Levenspiel, O., (1999). Chemical reaction engineering. Third Edition. *John Wiley and Sons* (pp. 13)
- Oinas, P., Wild, G., Midoux, N., & Haario, H. (1995). Identification of mass-transfer parameters in cases of gas absorption and chemical reaction. *Chemical Engineering and Processing* 34 (1995) 50% 5 13
- Olutoye, M. A. & Mohammed, A., (2006) Modelling of a Gas-Absorption Packed Column for Carbon Dioxide-Sodium Hydroxide System AU J.T. 10(2): 132-140
- Onda, K., Takeuchi H, & Okumoto, Y., (1968). "Mass transfer coefficients between gas and liquid phases in packed columns." *Journal of Chemical Engineering of Japan*. 1968; 1(1): 56-62.
- Onda, K., Sada, E., Murase, Y. (1959), "Liquid-side mass transfer coefficients in packed towers", *AIChE J.*, 5(2):235,1959
- Orhorhoro, K. E. & Atumah, V. E., (2018). Performance Evaluation of Design AD System Biogas Purification Filter. *International Journal of Mathematical Engineering and Management Science* Vol 3, No 1, 17-27, 2018. Retrieved uary 16, 2018 from www.ijmeme.in/assets/3-ijmeme-16-030-vol.-3%2C-no.-1%2C-17-27%2C-2018.pdf.
- Danckwerts, P. V. (1970). Gas-Liquid Reactions. New York, McGraw-Hill, **1970**, Chap.9, 206.
- Peleg, M., Normand, M. D. & Corradini, M. G., (2012): The Arrhenius Equation Revisited, *Critical Reviews in Food Science and Nutrition*, 52:9, 830-851
- Penteado, R. B, Hagui. T. G., Faria. J. C., Silva, M. B., & Ribeiro. M. V., (2016). Application of Taguchi Method in process improvement of turning of a superalloy *NIMONIC 80A*. Adopted on September 19, 2018 from <https://www.pomsmeetings.org>

- Perry, R. H., Green, D. W., (2008). Perry's Chemical Engineers' Hand Book Eighth Edition. McGraw-Hill, Inc. 2008.
- Pertiwiingrum, A., Harto, A. W., Wuri, M. A., & Budiarto, R., (2018). Assessment of Calorific Value of Biogas after Carbon Dioxide Adsorption Process Using Natural Zeolite and Biochar. *International Journal of Environmental Science and Development*, Vol. 9, No. 11, November 2018.
- Ulbig, P. & Hoburg, D., (2002). Determination of the calorific value of natural gas by different methods. Retrieved on March 16, 2018 from: <https://www.researchgate.net/publication/232379111>.
- Pinto, D. D. D., Emonds, R., & Versteeg, G. F. (2016). Experimental determination of mass-transfer coefficients and area of dumped packing using alkanolamine solvents. *Energy Procedia*, 86, 219-228. <https://doi.org/10.1016/j.egypro.2016.01.023>
- Pohorecki, R. & Moniuk, W. (1988). Kinetics of reaction between carbon dioxide and hydroxyl ions in aqueous electrolyte solutions. *Chemical Engineering Science*. Volume 43, Issue 7, 1988, Pages 1677-1684
- Power Africa. Development of Kenya's power sector 2015-2020" web site: https://www.usaid.gov/sites/default/files/documents/.../Kenya_Power_Sector_report.pdf. Retrieved on February 16, 2018.
- Pradeep, A., (2010). Numerical Methods in Chemical Engineering, *PHI Learning Private Limited*, 1st Edition, pp119
- Pragajibhai, D. H., Nalwaya, S., Singh, P. & Jain, R., (2018). Optimization of Machining Parameters on Surface Roughness by Taguchi Approach. *International Journal of Research and Scientific Innovation (IJRSI)* | Volume V, Issue IV, April 2018 | ISSN 2321-2705.
- Kasikamphaiboon, P., Chungsiriporn, J., Bunyakan, C., & Wiyaratn, W. (2013). "Simultaneous removal of CO₂ and H₂S using MEA solution in a packed column absorber for biogas upgrading" *Songklanakarinn J. Sci. Technol.* 35 (6), 683-691, Nov. - Dec. 2013
- Qafary, M., Gharanfoli, M. & Qafari, S. M., (2018). Taking Advantage of Taguchi Design Method to Optimize Medium Culture Conditions for Producing Recombinant Follicle Stimulating Hormone. *Journal of Biometrics & Biostatistics*, J Biom Biostat 2018, 9:4 DOI: 10.4172/2155-6180.1000409.
- Qing, Z., Yincheng, G., Zheng, N. & Lin, W., (2011). Mass Transfer Coefficients for CO₂ Absorption into Aqueous Ammonia Solution Using a Packed Column. Department of Engineering Mechanics, *Tsinghua University*, Beijing 100084, China. Retrieved on October 21, 2017 From pubs.acs.org/doi/abs/10.1021/ie101821b.
- Jain, R. & Gupta, N., (2017). Review on Orthogonal Collocation Method for Solving Ordinary Differential Equations. *JETIR* January 2017, Volume 4, Issue 1. Retrieved from www.jetir.org (ISSN-2349-5162 on October 2, 2019).
- Jain, R., (2017). Study of Solution of Second Order Differential Equations Using Orthogonal Collocation Method on Finite Elements. *IJCRT* | Volume 5, Issue 2 June 2017 | ISSN: 2320-2882
- Rau, F. A., Krause, H. H., Fino, R., Trimis, D., (2017) Production of hydrogen by Auto thermal reforming of biogas. *Energy Procedia* Volume 120, August 2017, Pages 294-301. Retrieved on December 23, 2017 from <https://doi.org/10.1016/j.egypro.2017.07.218>. Retrieved on August 13-2018 from <https://www.ethz.ch>lec3-6> .
- Fernández-Prini, R., Alvarez, J. L., Harvey, A. H., (2003). Henry's Constants and Vapor-Liquid Distribution Constants for Gaseous Solutes in H₂O and D₂O at High Temperatures. *J. Phys. Chem. Ref. Data*, Vol. 32, No. 2, 2003. Retrieved on August 17-2018 from www.satellite.mpic.de>henry-3.
- Rannacher, R., (1999). Finite Element Methods for the Incompressible Navier-Stokes. *Institute of Applied Mathematics* University of Heidelberg.: <http://gaia.iwr.uni-heidelberg>

- Roy, R. (1990). *A Primer on the Taguchi Method*. New York: Van Nostrand Reinhold.
- Nouh, S. A., Lau, K. K., & Shariff, A. M., (). Modelling and simulation of a fixed bed adsorption column using integrated CDF approach. *Journal of applied science* 10 (24): 3229-3235, 2010.
- Gheni, S. A., Mohammed F. Abed, Essam K. Halabia, Saad R. Ahmed. Investigation of carbon dioxide (CO₂) capture in a falling film contactor by computer simulation. *Oil & Gas Science and Technology - Revue d'IFP Energies nouvelles*, Institut Français du Pétrole, 2018, 73, pp.43. 10.2516/ogst/2018020. hal-01902841
- Sánchez, A. P.; Sánchez, E. J. P.; Silva, R. S, (2016). Design of a packed-bed absorption column considering four packing types and applying Matlab. *Nexo Revista Científica*/Vol. 29, No 02, pp 83-104/Diciembre 2016. <http://dx.doi.org/10.5377/nexo.v29i2.4577>
- Schiltes, M., (2018). Designing CO₂. Absorption Columns with Activated Amine Solutions. *Chemical Engineering Transactions* vol. 69, 2018. *The Italian Association of Chemical Engineering*. Online at www.aidic.it/cet.
- Schwaninger, M. & Hadjis, A., (1998), Model Building and Validation: Contributions of the Taguchi Method, *International System Dynamics Conference 1998*, Québec.
- Fogler, S. (1999). *Elements of chemical reaction engineering*. Prentice Hall International Editions. Third Edition. Retrieved on August 18-2018 from www.engin.umich.edu/~cre
- Sekulić, M., Gostimirović, M., Kovač, P. & Savković, B., (2011). Optimization of Cutting Parameters Based on Tool chip Interface Temperature in Turning Process Using Taguchi's Method. *15th International Research/Expert Conference "Trends in the Development of Machinery and Associated Technology" TMT 2011*, Prague, Czech Republic, 12-18 September 2011.
- Selvamony, S. C. B, (2018). Kinetics and Product Selectivity (Yield) of Second Order Competitive Consecutive Reactions in Fed-Batch Reactor and Plug Flow Reactor. *ISRN Chemical Engineering* Volume 2013, Article ID 591546, 17 pages <http://dx.doi.org/10.1155/2013/591546>.
- Seo, D. J. & Hong, W. H. (2000) "Effect of Piperazine on the Kinetics of Carbon Dioxide with Aqueous Solutions of 2-Amino-2-methyl-1-propanol". *Industrial and Engineering chemistry research*. Res., 2000, 39 (6), pp 2062–2067. pubs.acs.org/doi/abs/10.1021/ie990846f. Retrieved January 17-2018.
- Seyedeh Gita Sharafi, Rahabar Rahimi, Morteza Zivdar., 2017 Pressure Drop in a Randomly Packed Absorption Tower in Transient Flow Regime.
- Shabani A., Siamak T. A., & Shahraki, B. H. (2010). Calculation of effective interfacial area in a Turbulent Contact Absorber. *International Journal of Chemical Engineering and Applications*, Vol. 1, No. 1, June 2010. ISSN: 2010-0221 Retrieved on February 1,2018 from: ijcea.org/papers/20-A001.pdf
- Shafeeyan, M. S., Daud, W. M. A. W., Shamiri, A., (2014). A review of mathematical modeling of fixed-bed columns for carbon dioxide adsorption. *chemical engineering research and design* 92 (2014) 961–988
- Shahavi, M. H., Hosseini, M., Jahanshahi, M., Meyer, R. L. & Darzi, G. M. (2016). Clove oil nanoemulsion as an effective antibacterial agent: Taguchi optimization method. *Desalination and Water Treatment*. August 2016. DOI: 10.1080/19443994.2015.1092893. retrieved on May 26, 2021, from <http://www.tandfonline.com/loi/tdwt20>.
- Gondal, S., (2014) "Carbon dioxide absorption into hydrogen and carbonate systems". (Doctoral Dissertation, *Norwegian University of Science and Technology*, 2014) Retrieved from ISBN 978-82-326-0443-2 (electronic version)
- Arora, S. & Kaur, I., (2015). Numerical solution of heat conduction problems using orthogonal collocation on finite elements. *Journal of the Nigerian Mathematical Society* 34 (2015) 286–302. Retrieved from www.sciencedirect.com on December 5, 2019

- Dragan, S., (2016) "Calculation of the effective mass transfer area in turbulent contact absorber" *STUDIA UBB CHEMIA*, LXI, 3, Tom I, 2016 (p. 227-238)
- Somaskandan, V. & Muthukrisnan, V., (2015) Optimization of process parameter of wet scrubbing of biogas and vegetable waste using historical and Taguchi design. Article in *Process in Industrial Ecology*. An international Journal 2015
- Song, D., (2017). Effect of Liquid Viscosity on Liquid Film Mass Transfer for Packing. (Unpublished doctoral dissertation). *University of Texas Austin*, Austin, TX. USA
- Sonin, A. A., (2001). "The Physical Basis of dimensional analysis" Second Edition. Department of Mechanical Engineering *MIT* Cambridge, MA 02139.
- Dixit, O., (2015). Upgrading Biogas to Biomethane Using Absorption. PhD Dissertation. *Technische Universität Dresden*
- Kotsiantis, S., Kanellopoulos, D. (2006). Discretization Techniques: A recent survey *GESTS International Transactions on Computer Science and Engineering*, Vol.32 (1), 2006, pp. 47-58
- Stefan, S., & Mazzotti, M., (2018). Introduction to Chemical Engineering for Lectures 3-6: Thermodynamics. *ETH Zurich, Institute of Process Engineering*, Sonneggstrasse 3, CH-8092 Zurich, Switzerland.
- Stolaroff, J. K., Keith, D. W. & Lowry, G. V., (2008). Carbon dioxide capture from atmospheric air using sodium hydroxide spray: Supporting Information. *Environmental Science and Technology*.
- Sudhakara, D. & Prasanthi, G., (2014). Application of Taguchi Method for Determining Optimum Surface Roughness in Wire Electric Discharge Machining of P/M Cold Worked Tool Steel (Vanadis-4E). *Procedia Engineering* 97 (2014) 1565 – 1576. 12th Global Congress on Manufacturing and Management, GCM 2014.
- Taguchi, G., & Konishi, S., (1987). Taguchi Methods, orthogonal arrays and linear graphs, tools for quality American supplier institute, *American Supplier Institute*; 1987 [p. 8-35]
- Tan, L. S, Shariff, A. M, Lau, K. K. & Bustam, M. A, 2012. Factors affecting CO₂ absorption efficiency in packed column: A review. *Journal of Industrial and Engineering Chemistry* 18 (2012) 1874–1883. Retrieved on November 20, 2019 from <https://www.researchgate.net/publication/271614667>
- Tavan, Y., & Hosseini, S. H., (2017). A novel rate of the reaction between NaOH with CO₂ at low temperature in spray dryer. *Petroleum* 3 (2017) 51e55.
- Theodoros, D., Athanasios, Papadopoulos, I. & Panos (2014). Solvent based Post Combustion CO₂ Capture Flowsheet through Generalized Modelling Framework. *Clean Technologies and Environmental Policy* October 2014, Volume 16. Issue 7, pp 1363-1380. DOI:10.1007/s10098-0747-2. Online ISSN 1618-9558
- Tontiwachwuthikul, P., Meisen, A. & Jim, L. C., (1992). CO₂ absorption by NaOH, Monoethanolamine and 2-amino-2-methyl-1-propanol solutions in a packed column. *Chemical Engineering Science* Volume 47, Issue 2, February 1992, Pages 381-390. Retrieved on October 27, 2017 from [https://doi.org/10.1016/0009-2509\(92\)80028](https://doi.org/10.1016/0009-2509(92)80028)
- Tsai, H. H., Wu, D. H., Chiang, T. L., & Chen, H. H. (2009) Robust Design of SAW Gas Sensors by Taguchi Dynamic Method *Sensors* 2009, 9, 1394-1408; doi:10.3390/s90301394
- Tsai, R. (2010). Mass Transfer Area of Structured Packing. Doctoral Dissertation, *the University of Texas at Austin*, 2010.
- United Nations Climate Change (1998). Kyoto protocol to the united nations framework convention on climate change 1998. Retrieved on February 5, 2018 From <https://unfccc.int/resource/docs/convkp/kpeng.pdf>.

- United States Environmental Protection Agency (January 19, 2017). Contribution of Working Group III to the Fifth Assessment Report of the Intergovernmental Panel on Climate. Retrieved on February 16, 2018 from: <https://www.epa.gov/ghgemissions/global-greenhouse-gas-emissions-data>
- USDL-United States Department of Labor Occupational Safety and Health Administration. Retrieved on February 5, 2018 from: <https://www.osha.gov/SLTC/hydrogensulfide/hazards.html>.
- van Elk, E. P., Knaap, M. C. & Versteeg, G. F., (2007). Application of the penetration theory for gas-liquid mass transfer without liquid bulk –Differences with Systems with a Bulk. *Chemical Engineering Research and Design*. Retrieved on October 27, 2017. From <https://www.rug.nl/research/portal/files/14491991/2007ChemEngResDesVanElk.pdf>.
- van Holst, J., Versteeg, G. F., Brillman, D. W. F. & Hogendoorn, J. A., (2009). Kinetic study of CO_2 with various amino acid salts in aqueous solution. *Chemical Engineering Science* 64 (2009) 59 – 68.
- Vijay, V.K., Chandra, R., Subbarao, P.M.V., & Kapdi, S. S., (2006). Biogas Purification and Bottling into CNG Cylinders: Producing Bio-CNG from Biomass for Rural Automotive Applications. *The 2nd Joint International Conference on "Sustainable Energy and Environment"*, 21-23 November, Bangkok. Retrieved on January 12, 2018 From: [www.valorgas.soton.ac.uk/.../120825_VALORGAS_241334_D5-2_rev\[0\].pdf](http://www.valorgas.soton.ac.uk/.../120825_VALORGAS_241334_D5-2_rev[0].pdf).
- Villanueva, P. E., Antonio-Abdu, S. & Magomnang, M., (2014). Removal of Hydrogen Sulfide from Biogas using Dry Desulfurization Systems. *International Conference on Agricultural, Environmental and Biological Sciences (AEBS-2014)* April 24-25, 2014 Phuket (Thailand) Retrieved on February 5, 2018 From: iicbe.org/upload/3607C414016.pdf.
- Volker, J., Matthies, G., & Rang, J., (2005). A comparison of time-discretization/linearization approaches for the incompressible Navier–Stokes equations. *Computer Methods Appl. Mech. Engrg.* 195 (2006) 5995–6010.
- Wang, C. (2015). Mass Transfer Coefficients and Effective Area of Packing (Doctoral dissertation, The University of Texas at Austin, 2015). Dissertation abstract.
- Wang, C., Perry, M., Rochelle, G. T., Seibert, A. F., (2012). Packing characterization: Mass Transfer Properties. *Energy Procedia* 23 (2012) 23 – 32. Trondheim CCS Conference-6. Available online at www.sciencedirect.com.
- Grande, G. A., (2014). Biogas Upgrading by Pressure Swing Adsorption. *Biofuel's Engineering Process Technology*. <https://www.researchgate.net/publication/221914229>
- Wen, J., Shi, K., Sun, Q., Sun, Z. and Gu, H., (2018). Measurement for Surface Tension of Aqueous Inorganic Salt. *Front. Energy Res.* 6:12. doi: 10.3389/fenrg.2018.00012
- Whitman, W. G., (1923). The Two-Film Theory of Gas. *Chemical and Metallurgical Engineering*. Vol. 29, No. 4.
- Wilke and Chang (1955). Coefficients in dilute solutions. University of California, Berkeley, California www.sciencedirect.com/science/article/pii/0009250955850075/pdf?md5.
- Xiao, S., Sun, W., Du, J. & Li, G. (2014). Application of CFD, Taguchi Method, and ANOVA Technique to Optimize Combustion and Emissions in a Light Duty Diesel Engine. *Hindawi Publishing Corporation Mathematical Problems in Engineering*, Volume 2014, Article ID 502902, 9 pages. <http://dx.doi.org/10.1155/2014/502902>
- Xiao-xiong, Z., Jia-qian, N. & XU, B., (2017). Meso-scale CFD Modelling of CO₂ Capture by Aqueous Ammonia Part I: Modeling. *2nd International Conference on Applied Mathematics, Simulation and Modelling (AMSM 2017)* ISBN: 978-1-60595-480-6

- Xu, B., Gao, H., Huiyingi, X., & Liang, Z., (2012). Mass transfer performance of CO₂ absorption into aqueous DEEA in packed columns. *International Journal of Greenhouse Gas Control* Volume 51, Pages 11-17.
- Haroun, Y., Raynal, L., Legendre, D., (2013). Mass transfer and liquid hold-up determination in structured packing by CFD DOI: 10.1016/j.ces.2012.03.011 <http://dx.doi.org/10.1016/j.ces.2012.03.011>
- Yacine, H., & Ludovic, R (2016) Use of Computational Fluid Dynamics for Absorption Packed Column Design. *Oil Gas Science and Technology - Revue d'IFP Energies nouvelles*, Institut Français du Pétrole, 2016, 71 (3), ff10.2516/ogst/2015027ff. fffhal-01395112f
- Yang, B., Lai, Y., Yue, X., Wang, D. & Zhao, Y. (2020). Parametric Optimization of Laser Additive Manufacturing of Inconel 625 Using Taguchi Method and Grey Relational Analysis. *Hindawi Scanning* Volume 2020, Article ID 9176509, 10 pages <https://doi.org/10.1155/2020/9176509>
- Yang, Q., Puxty, G., Susan, J., Brown, M., Feron, P. & Conway, W., (2014). Toward Intelligent CO₂ Capture Solvent Design through Experimental Solvent Development and Amine Synthesis. *Industrial and Engineering Chemistry research*. Retrieved on October 24,2017, from: <http://pubs.acs.org/doi/abs/10.1021/acs.energyfuels.6b00875>.
- Yincheng, G., Wenyi, L. & Niu, Z. (2011). Comparison of removal efficiencies of carbon dioxide between aqueous ammonia and NaOH solution in a fine spray column. *Energy Procedia* Volume 4, 2011, Pages 512-518. Retrieved on October 21,2017 From: <https://www.sciencedirect.com/science/article/pii/S1876610211000000/pdf?md5=1-s2.0.1>.
- Yoo, M., Sang-Jun, H., Jung-Ho, W., (2013). Carbon dioxide capture capacity of sodium hydroxide aqueous solution. *Journal of Environmental Management* 114 (2013) 512e519
- Sovilj, M. N., Nikolovski, B. G , Spasojević, M. D, Mauhar, S. M. (2019). Packed Bed Absorption Column: Hydrodynamics and Mass Transfer. *APTEFF*, 50, 1-352 (2019) UDC: 532.5:533.6.011:66.021.3 DOI: <https://doi.org/10.2298/APT1950260S>
- Charpentier, J. C., (1976). Recent Progress in Two Phase Gas-Liquid Mass Transfer in Packed Beds. *The Chemical Engineering Journal*, II (1976) 161-181
- Zakeria, A., Einbub, A., Wiigb, P. O., Øic, L. E. & Svendsena, H. F. (2011), Experimental Investigation of Pressure Drop, Liquid Hold-Up and Mass Transfer Parameters in a 0.5 m Diameter Absorber Column. *Energy Procedia* 4 (2011) 606–613 Retrieved on March 10, 2018 from: www.sciencedirect.com.
- Zha, X., Ning, J., & XU, B., (2017). 2nd International Conference on Applied Mathematics, Simulation and Modelling (AMSM 2017). ISBN: 978-1-60595-480-6.

**

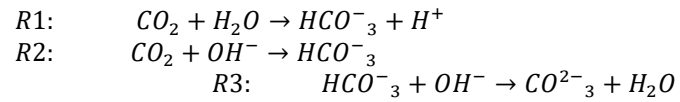
APPENDICES

Appendix A: Parameters for the solvent.

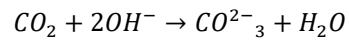
Solvent Concentration [OH ⁻] (<i>gmol</i> · <i>L</i> ⁻¹)	Viscosity μ , (cP)	Diffusion Coefficient, $D_{CO_2,x}$ (<i>m</i> ² · <i>s</i> ⁻¹)	Henry's Law constant, H_{cp} (<i>kmol</i> · <i>m</i> ⁻³ · <i>Pa</i> ⁻¹)	Second-order reaction rate constant, k_1 (<i>m</i> ³ · <i>kmol</i> ⁻¹ · <i>s</i> ⁻¹)
0.1	1.0374	1.6E - 6	0.03535	4.0832
0.2	1.0748	1.6E - 6	0.03410	4.2708
0.3	1.1122	1.6E - 6	0.03325	4.6465
0.4	1.1496	1.6E - 6	0.03205	4.6646
0.5	1.1870	1.6E - 6	0.03095	4.8708
0.6	1.2244	1.6E - 6	0.02680	5.0833
0.7	1.2618	1.6E - 6	0.02995	5.3023
0.8	1.2992	1.6E - 6	0.02805	5.5275
0.9	1.3366	1.6E - 6	0.02715	5.7592
1.0	1.370	1.6E - 6	0.02635	5.9972

Appendix B: Gas-Solvent reaction mechanism

The major reaction in the absorption column is that of carbon dioxide and sodium hydroxide. This reaction has been studied widely. It can be expressed as follows:



At a pH greater than 10, reaction *R1* has a negligible effect on the rate of carbon dioxide absorption. The next reaction *R2* is followed by an instantaneous reaction *R3*. Therefore, the overall reaction between carbon dioxide and aqueous sodium hydroxide solution can be expressed as:



This is a second first order irreversible reaction.

Appendix C: The $L_9(3^4)$ Orthogonal Array

Experiment Number	Independent Variables.				Averaged Performance Parameters	
	u_y	u_x	$[OH^-]$	y_a	y_b	$K_y a_e$ ($kmol/m^2 \cdot s \cdot kPa$)
1	1	1	1	1	0.0808	0.099017
2	1	2	2	2	0.0104	0.022335
3	1	3	3	3	0.0001	0.491151
4	2	1	2	3	0.2014	0.035657
5	2	2	3	1	0.1080	0.246973
6	2	3	1	2	0.0610	0.363912
7	3	1	3	2	0.2784	0.168839
8	3	2	1	3	0.2206	0.263379
9	3	3	2	1	0.0940	0.451447

Appendix D: The column simulation code

```

#include <iostream>
#include <ctime>
#include <stdlib.h>
using namespace std;
double u, r, dif, H, z, k, oh, Y, e;
void solve(double* a, double* b, double* c, double* d, int n)
{
    n--; // since we start from x0 (not x1)
    c[0] /= b[0];
    d[0] /= b[0];
    for (int i = 1; i < n; i++)
    {
        c[i] /= b[i] - a[i]*c[i-1];
        d[i] = (d[i] - a[i]*d[i-1]) / (b[i] - a[i]*c[i-1]);
    }
    d[n] = (d[n] - a[n]*d[n-1]) / (b[n] - a[n]*c[n-1]);
    for (int i = n; i-- > 0;)
    {
        d[i] -= c[i]*d[i+1];
    }
}
int main()
{
    system("color 2E");
    time_t now = time(0);
    char * dt = ctime(&now);
    std::cout << "\t\t" << dt << std::endl;
    std::cout << "\tEnter the gas superficial velocity:";
    std::cin >> u;
    std::cout << "\tEnter the solvent concentration in gmol/L:";
    std::cin >> oh;
    if(oh = 0.1)
        k = 8.3455;
    std::cout << "\tEnter the inlet CO2 mole fraction:";
    std::cin >> Y;
    int e = 10;
    double dif = 0.00016;
    int n = e+1;
    std::cout << "\t\tSolution of the CDR equation " << std::endl;
    std::cout << "\t\t=====\n\n" << std::endl;
    std::cout << "\tNumber of elements:" << e << std::endl;
    std::cout << "\n\tNode Number\tx(meters)\tSolute Mole Fraction" << std::endl;
    std::cout << "\t-----\t-----\t-----" << std::endl;

    double h = 0.35;
    double z = h/e;
    double A = (dif/(z*z)+(u/z));
    double AN = (2*dif/(z*z)+(u/z);
    double B1 = -(2*dif/(z*z))-(3*u/z)-(k*oh)-(2*u*u/dif);
    double B = -(2*dif/(z*z))-(u/z)-k*oh;
    double C1 = (2*dif/(z*z)+(u/z));
    double C = dif/(z*z);
    double R1 = -(((2*u*u)/dif)+((2*u)/z))*Y;
    double R = 0;
    double a[11] = { A, A, A, A, A, A, A, A, A, AN};

```

```
double b[11] = { B1, B, B, B, B, B, B, B, B, B, B};
double c[11] = { C1, C, C, C, C, C, C, C, C, C, C};
double d[10] = { R1, R, R, R, R, R, R, R, R, R};
    solve(a,b,c,d,n);
        for (int i = 0; i < n; i++)
            {
                cout << "\t\t\t\t\t" << d[i] << endl;
            }
return 0;
}
```

**